GLOBAL PRECIPITATION MEASUREMENT (GPM) MISSION

Algorithm Theoretical Basis Document

GPROF2017 Version 1 (used in GPM V5 processing)

June 1st, 2017

Passive Microwave Algorithm Team Facility

TABLE OF CONTENTS

GLOSSARY OF ACRONYMS

A

Advanced Microwave Scanning Radiometer for the Earth observing system (AMSR-E)

Advanced Microwave Sounding Unit (AMSU)

ATBD (Algorithm Theoretical Basis Document)

C

Colorado State University (CSU)

D

Dual Frequency Radar (DFR)

E

European Centre for Medium-Range Weather Forecasts (ECMWF)

G

GANAL (JMA Global ANALysis)

GPM (Global Precipitation Measurement)

GPM Microwave Imager (GMI)

GPM Profiling Algorithm (GPROF)

Global Data Assimilation System (GDAS)

Ground Validation (GV)

L

Land Surface Model (LSM)

N

National Centers for Environmental Prediction (NCEP)

Numerical weather prediction (NWP)

P

Precipitation Processing System (PPS)

Passive microwave retrieval (PWR)

Precipitation radar (PR)

T

Brightness temperature (T_b)

Tropical Rainfall Measuring Mission (TRMM)

Tropical Rainfall Measuring Mission - Microwave Imager (TMI)

1.0 INTRODUCTION

1.1 OBJECTIVES

The Global Precipitation Measurement (GPM) Mission is an international space network of satellites designed to provide the next generation precipitation observations every two to four hours anywhere around the world. GPM consists of both a defined satellite mission and a collaborative effort involving the global community. The GPM concept centers on the deployment of a "Core" observatory carrying advanced active and passive microwave sensors in a non-Sun-synchronous orbit to serve as a physics observatory to gain insights into precipitation systems and as a calibration reference to unify and refine precipitation estimates from a constellation of research and operational satellites. As a science mission with integrated applications goals, GPM will advance understanding of the Earth's water and energy cycle and extend current capabilities in using accurate and timely information of precipitation to directly benefit the society. This current Algorithm Theoretical Basis Document (ATBD) deals with the Passive Microwave Algorithms associated with the GPM mission. The passive microwave algorithm is designed to take advantage of the Core observatory to define *a-priori* databases of observed precipitation profiles and their associated brightness temperature signals. These databases are then used in conjunction with Bayesian inversion techniques to build consistent retrieval algorithms for the Core satellite's GMI instrument and each of GPM's constellation satellites.

1.2 PURPOSE

This ATBD describes the Global Precipitation Measurement (GPM) passive microwave rainfall algorithm, which is a parametric algorithm used to serve all GPM radiometers. The output parameters of the algorithm are enumerated in Table 1. It is based upon the concept that the GPM core satellite, with its Dual Frequency Radar (DPR) and GPM Microwave Imager (GMI), will be used to build a consistent *a-priori* database of cloud and precipitation profiles to help constrain possible solutions from the GMI radiometer beyond the swath of the radar as well as the constellation radiometers.

In particular, this document identifies the physical theory upon which the algorithm is based and the specific sources of input data and output from the retrieval algorithm. The document includes implementation details, as well as the assumptions and limitations of the adopted approach. Because the algorithm is being developed by a broad team of scientists, this document additionally serves to keep each developer abreast of all the algorithm details and formats needed to interact with the code. The version number and date of the ATBD will, therefore, always correspond to the version number and date of the algorithm—even if changes are trivial.

Table 1. Key output parameters from the Level 2 Rainfall Product.

Pixel Information		
Parameter	**Units**	**Comments**
Latitude, longitude, Time	Deg.	Pixel earth coordinate position, and Pixel time
Surface Type	None	land surface emissivity class/ocean/coast/sea ice
Retrieval Type	None	Identifies if pixel retrieved with S0, S1, or S2
Pixel Status	None	Identifies pixels eliminated by QC procedures
Quality Flag	None	Pixels w/o good T_b matches in database
2 meter Surface Temperature Total Column Water Vapor Surface skin temperature	^oK mm ^oK	Pass-through variables from Model
Surface Precipitation	mm/hr	Total Precipitation
Frozen Precipitation Convective Precipitation	mm/hr mm/hr	Frozen Precipitation – grauple and snow Convective Precipitation - from DPR precip type
Precipitation structure	None	On/Off flag for self-similar hydrometeor profiles; 28 layers, separated by hydrometeor species
Precipitation Diagnostics	None	Precip Retrieval diagnostics and uncertainties
Cloud, Rain, Ice Water Paths	Kg/m^2	Integrated from retrieved DPR profile

1.3 SCOPE

This document covers the theoretical basis for the at-launch passive microwave algorithm used by GPM for the retrieval of liquid and solid precipitation from the GMI and constellation radiometers. It also describes the latest version of the input datasets, and GPROF algorithm which is in operational use at NASA's Precipitation Processing System (PPS).

The GPM radiometer algorithm is a Bayesian type algorithm. These algorithms search an *a-priori* database of potential rain profiles and retrieve a weighted average of these entries based upon an uncertainty weighted proximity of the observed T_b to the simulated T_b corresponding to each rain profile. By using the same *a-priori* database of rain profiles, with appropriate simulated T_b for each constellation sensor, the Bayesian method is completely parametric and thus well suited for GPM's constellation approach. The *a-priori* information supplied by GPM's core satellite immediately benefits not just the GMI radiometer but all radiometers that form GPM constellations. Because the ultimate objective is to use the DPR and GMI on the GPM core satellite to build this a-priori database, an alternative method to create the database had to be developed for the at-launch algorithm. It is understood that this is not the ideal method but it should be useful to test the truly parametric nature of the algorithm and provide rainfall estimates no worse than our best methods available today.

The mathematics of Bayesian inversions are well understood. The solution provides a mean rain rate as well as its uncertainty. The major sources of systematic errors in these algorithms are the quality of the *a-priori* database; the estimate of the forward model uncertainty; and the ancillary information used to subset the *a-priori* database.

Section 1 describes the objectives, purpose and scope of the document. Section 2 provides GPM satellite instrumentation background as well as a list of Constellation radiometers being considered. Details of the constellation radiometers are found in Appendix A. The process concepts and algorithm descriptions for the geophysical parameters of the rainfall product are presented in Section 3. Section 4 describes the algorithm infrastructure, while Section 5 summarizes the assumptions and limitations and Section 6 discusses the various planned algorithm improvements.

1.4 CHANGES FROM PREVIOUS VERSIONS – GPM V5 Release Notes

This ATBD represents version V1 of the GPROF2017 algorithm delivered to the Precipitation Processing System on May 1st, 2017. This is GPROF for GPM V5 version. As such, it contains details of what was implemented in the "working" version of the algorithm code. The code is parametric to a very large extent, requiring only that channel frequencies, polarizations and uncertainties be entered for each conically scanning radiometer. Cross-track sounder algorithms are constructed in nearly the same fashion but the addition of large scan angle variations is best handled by separate code that will be described in a separate section. Below are the actual Release Notes for this version.

Release Notes for GPROF for GPM V5 Public Release – May 1, 2017

The Goddard Profiling Algorithm is a Bayesian approach that nominally uses the GPM Combined algorithm to create it's a-priori databases. Given the importance of these databases to the final product, they are worth reviewing before discussing particular changes to the algorithm. GPROF V03 was implemented at the launch of the GPM mission and thus had no databases from the GPM satellite itself. Instead, databases were made from a combination of TRMM, Cloudsat, ground based radars and models. V4 used the GPM generated databases but had a very short lead time as the radar and combined algorithm were in flux until nearly the date of the public release. Because the V04 of the Combined algorithm appeared to significantly overestimate precipitation over land, the a-priori databases were constructed from the Combined Algorithm (V4) over ocean, but the DPR Ku (V4) over land and coastal regions. The very short lead time to produce the a-priori databases led to insufficient testing of GPROF for GPM V4 that resulted in some less-than ideal retrievals.

GPROF for GPM V5 retains the previous version (i.e. GPM V4) of the Combined and DPR-Ku products for its databases. Future versions of GPROF, because of its need for existing GPM products to construct it's a-priori database, will always be one version behind the Combined algorithm. In GPROF for GPM V5, we nonetheless improved some of the ice hydrometeor simulations in order to get better agreement between computed and simulated brightness temperatures [ref Sarah]. This leads to smaller bias adjustments in the radiometer simulations and to an overall better fit between the radiometer retrievals and both the Combined products as well as ground validation data.

GPROF for GPM V5 made additional changes to retrievals of high latitude oceanic drizzle and snowfall over land. Both of these changes were made because the DPR sensitivity of 12 dBZ was shown to miss substantial amounts of drizzle and light to moderate snowfall events. Because the GPM radars do not have signal in these cases, they are not addressed in the newer versions of the Combined and Radar products either.

Drizzle was addressed in the a-priori database by setting a threshold in the cloud liquid water retrieval from GMI (done before the DPR or Combined rainfall is inserted into the scene), to match the CloudSat based probability of rainfall. This is done for each temperature and Total Precipitable Water (TPW) bin used to subset the a-priori database. While this assumes that higher cloud liquid water amounts correspond to precipitation, the assumption is generally thought to be reasonable. Additional cloud water beyond the CloudSat determined threshold was partitioned between Cloud- and rain water similar to the procedure used by Hilburn and Wentz (2008). This increases rain water at high altitudes to agree better with CloudSat and ERA and MERRA re-analyses but continues to be low relative to these estimates. More work in ongoing to assess high latitude drizzle from different sources.

Over land, the US based MRMS data was used to build a-priori databases for snow covered surfaces of each of the constellations radiometers. Two years of MRMS data were matched up with individual satellite overpasses. This removed much of the low bias that GPROF for GPM V4 had over snow covered surfaces. **Because the MRMS data was only 2D and did not contain the vertical hydrometeor profiles, no profile information is available from the GPROF retrieval over snow covered surfaces.**

A final modification made to V4 is the determination of a precipitation threshold. Whereas GPROF for GPM V4 reported an unconditional rain rate and a probability of precipitation, it was up to the user to set a threshold (either in probability or rain rate) if rain/no rain information was needed. While GPROF for GPM V5 reports the same information, the algorithm has internally decided if the pixel is precipitating or not, and non-precipitating pixels have been set to zero rainfall. While the original probability of precipitation is still reported, its purpose is only as a diagnostic tool. The user can treat positive rainfall rates as definitively raining. Setting thresholds for precipitation is sometimes difficult in the snowfall where the radiometric information is very limited – particularly for sensors such as AMSR2 that lack high frequency channels. A new quality flag = 2 in therefore introduced.
Quality Flag = 0 still implies that the pixel is good. Quality flag = 1 means there are issues with the retrieval that require caution on the part of the user – particularly for applications such as constructing climate data records. Quality flag = 2 implies the rain/no rain threshold may not be working properly. When the quality flag is set to 3, the retrieved pixel should be used with extreme caution. A complete description of the GPROF quality flag is given below.

Limited validation done by the GPM Validation team shows significantly better correlations and smaller biases with GPROF for V5 than V4. Statistics were run over the Continental United States, Middleton, AK, and over a dense set of rain gauges in the Mountains of Austria. Even more limited validation have been done on snow due to the difficulty in getting reliable ground based measurements. Over the Olympic peninsula (GPM Field Experiment), the total precipitation over the mountains appears correct, but the phase is not. The phase of precipitation

in GPROF cannot be determined from the Tb signal itself. Instead, it is determined from the 2 meter temperature and dew point depression (provided by the ancillary data) according to Sims and Liu (2015). Because grid boxes of GANAL or ECMWF are relatively large, they do not capture small-scale terrain variability. Users needing to account for high resolution terrain variability will have to do so as post-processing step in V5. We hope to correct this in V6.

Almost no validation has been done on the constellation radiometer beyond comparisons of limited coincident overpasses with GMI, and comparisons of monthly means to ensure that the retrieval is performing as expected. AMSR2 comparisons against limited GV observations has similar statistics as GMI for liquid precipitation.

The GPROF output file has a parameter labeled 'CAPE'. This parameter is set to missing in GPROF V05. It will be used and implemented in subsequent versions.

GPROF 2017 V1 (GPM V5) Quality Flag Description

The GPROF Quality Flag variable for GPM V5 has added one additional index. The old indices in V3 and V4 included values: 0,1,2. The new index can be 0,1,2,3

The description is as follows:

Value 0: pixel is "good" and has the highest confidence of the best retrieval.

Value 1: "use with caution" . Pixels can be set to value 1 for the following reasons:

1) Sunglint is present, RFI, geolocate, warm load or other L1C 'positive value" quality warning flags
2) All sea-ice covered surfaces
3) All snow covered surfaces
4) Sensor channels are missing, but not critical ones.

Value 2: "use pixel with extreme care over snow covered surface" This is a special value for snow covered surfaces only. The pixel is set to 2 if the probability of precipitation is of poor quality or indeterminate. Use these pixels for climatological averaging of precipitation, but not for individual storm scale daily cases.

Value 3: "Use with extreme caution". Pixels are set to value 3 if they have channels missing critical to the retrieval, but the choice has been made to continue the retrieval for these pixels.

Hilburn, K.A. and F.J. Wentz, 2008: Intercalibrated Passive Microwave Rain Products from the Unified Microwave Ocean Retrieval Algorithm (UMORA). *J. Appl. Meteor. Climatol.,* **47**, 778–794, doi: 10.1175/2007JAMC1635.1.

Sims, E.M. and G. Liu, 2015: A Parameterization of the Probability of Snow–Rain Transition. *J. Hydrometeor.,* **16**, 1466–1477, doi: 10.1175/JHM-D-14-0211.1.

2.0 INSTRUMENTATION

2.1 GPM CORE SATELITE

The GPM Core Spacecraft will fly two precipitation instruments: the GPM Microwave Imager (GMI) and the Dual-frequency Precipitation Radar (DPR). Together, these instruments will provide a unique capability for measuring precipitation falling as light rain or snow—conditions that have been difficult to detect using previous instruments. Compared to the earlier generation of instruments, the new capabilities of the GMI and DPR are enabled by the addition of high frequency channels (165.6 and 183.3 GHz) on the GMI, and the inclusion of a Ka-band (35.5 GHz) radar on the DPR.

2.1.1 GPM Microwave Imager

The GPM Microwave Imager (GMI) instrument is a multi-channel, conical-scanning, microwave radiometer serving an essential role in the near-global-coverage and frequent-revisit-time requirements of GPM (see Fig. 1). The instrumentation enables the Core spacecraft to serve as both a 'precipitation standard' and as a 'radiometric standard' for the other GPM constellation members. The GMI is characterized by thirteen microwave channels ranging in frequency from

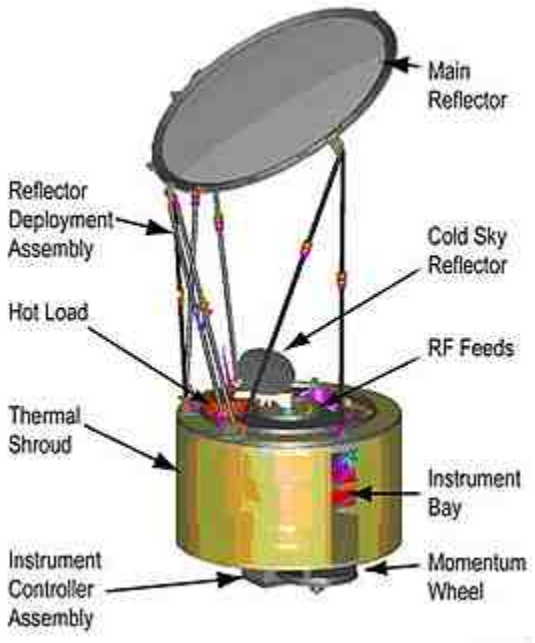

Fig. 1. GMI instrument.

10 GHz to 183 GHz (see Table 2). In addition to carrying channels similar to those on the Tropical Rainfall Measuring Mission (TRMM) Microwave Imager (TMI), the GMI carries four high frequency, millimeter-wave channels at about 166 GHz and 183 GHz. With a 1.2 m

diameter antenna, the GMI will provide significantly improved spatial resolution over TMI. Launch date for the core spacecraft: February, 2014.

Table 2. GMI performance characteristics.

Frequency (GHz)	Polarization	NEDT/ Reqmt (K)	Expected* NEDT	Expected Beam Efficiency (%)	Expected Calibration Uncert.	Resolution (km)
10.65	V/H	0.96	0.96	91.4	1.04	32.1 x 19.4
18.7	V/H	0.84	0.82	92.0	1.08	18.1 x 10.9
23.8	V	1.05	0.82	92.5	1.26	16.0 x 9.7
36.64	V/H	0.65	0.56	96.6	1.20	15.6 x 9.4
89.0	V/H	0.57	0.40	95.6	1.19	7.2 x 4.4
166.0	V/H	1.5	0.81	91.9	1.20	6.3 x 4.1
183.31±3	V	1.5	0.87	91.7	1.20	5.8 x 3.8
183.31±7	V	1.5	0.81	91.7	1.20	5.8 x 3.8

2.1.2 Dual-Frequency Precipitation Radar

One of the prime instruments for the GPM Core Observatory is called the Dual-frequency Precipitation Radar (DPR). The DPR consists of a Ku-band precipitation radar (KuPR) and a Ka-band precipitation radar (KaPR). The KuPR (13.6 GHz) is an updated version of the highly successful unit flown on the TRMM mission. The KuPR and the KaPR will be co-aligned on the GPM spacecraft bus such that the 5-km footprint location on the Earth will be the same. Data collected from the KuPR and KaPR units will provide the 3-dimensional observation of rain and will also provide an accurate estimation of rainfall rate to the scientific community. The DPR instrument will be allocated 190 Kbps bandwidth over the 1553B spacecraft data bus. The collection of the DPR data will be transmitted to the ground using the TDRSS multiple access (MA) and single access (SA) services.

The DPR is a spaceborne precipitation radar capable of making accurate rainfall measurements. The DPR is more sensitive than its TRMM predecessor especially in the measurement of light rainfall and snowfall in the high latitude regions. Rain/snow determination is accomplished by using the differential attenuation between the Ku-band and the Ka-band frequencies. The variable pulse repetition frequency (VPRF) technique is also expected to increase the number of samples at each IFOV to realize a 0.2 mm/h sensitivity.

The KuPR and KaPR, together with GMI, are the primary instruments on the GPM spacecraft. These Earth-pointing KuPR and KaPR instruments will provide rain sensing over both land and ocean, both day and night. Top-level general design specifications are seen in Table 3 and Fig. 2.

Table 3. DPR performance characteristics.

Item	Swath Width (km)	Range Resolu-tion (m)	Spatial Resolu-tion (km Nadir)	Beam Width (deg)	Trans-mitter (SSA)	Peak Transmit Power (W)	Pulse Repe-tition Freq. (Hz)	Pulse Width	Beam #
KuPR	245	250	5	0.71	128	1000	4100 - 4400	2; 1.667 μs pulses	49
KaPR	120	250/500	5	0.71	128	140	4100 - 4400	2; 1.667 μs pulses in matched beams 2; 3.234 μs pulses in interlaced scans	49 (25 matched beams and 24 interlaced scans)

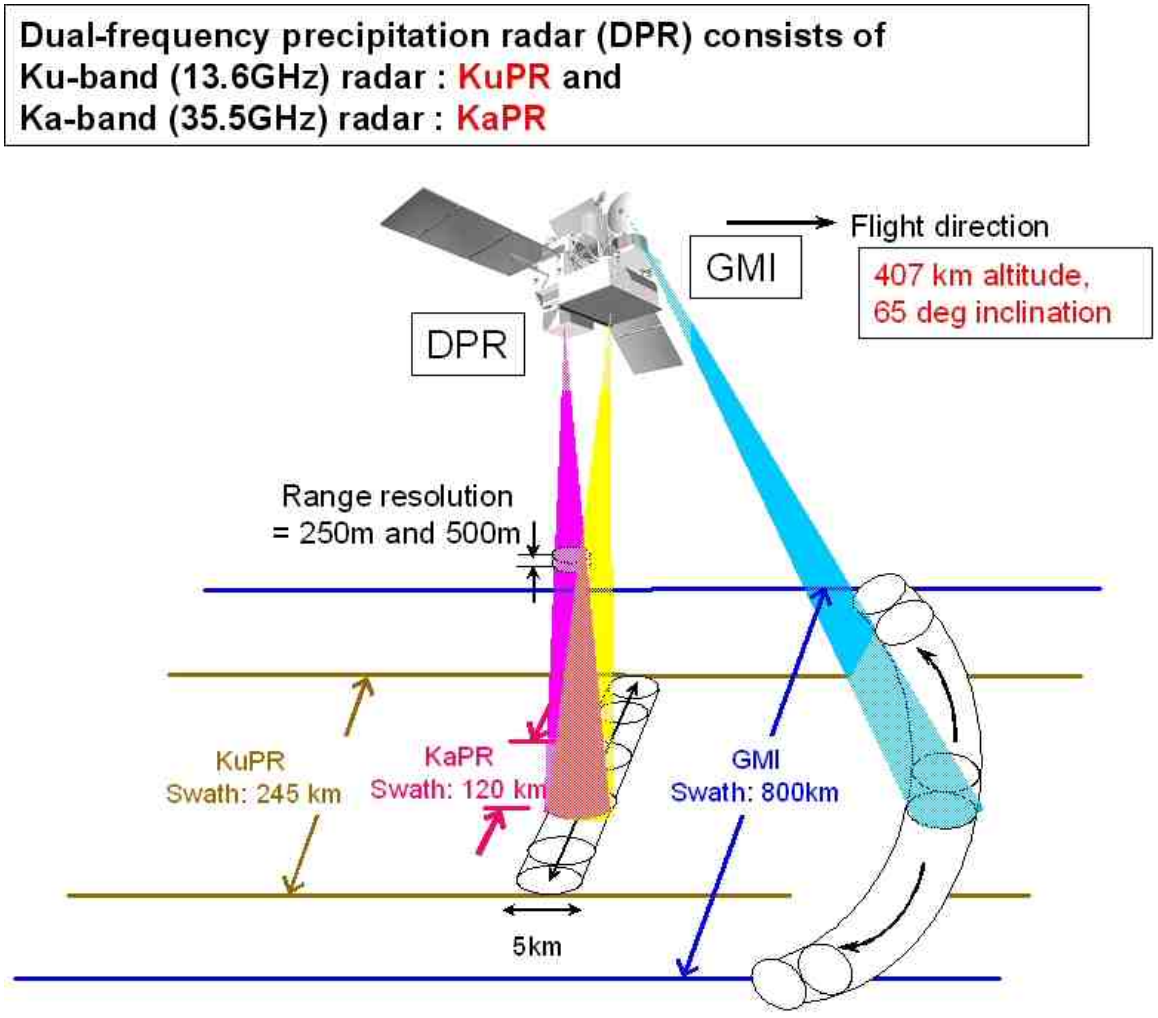

Fig. 2. GPM swath measurements.

2.2 GPM CONSTELLATION SATELLITES

In addition to the core instruments (GMI and DPR) the passive microwave algorithm will make use of several constellation radiometers that have similar channel sets as the GMI radiometer. These constellation radiometers are listed in Table 4 and described in detail in Appendix A.

Table 4. Launch and end dates of constellation radiometers in order of launch

Constellation Radiometers	**Launch Date**	**End Date**
AMSR 2	May 18th, 2012	Active
SAPHIR	End of 2010	N/A
SSMIS	-F-16: Oct. 18, 2003	Active
	-F-17: Nov. 4, 2006	Active
	-F-18: Oct. 18, 2009	Active
WindSat	Jan. 6, 2003	Active
AMSR-E	May 4, 2002	Oct, 2011
*AMSU A	NOAA-15 (NOAAK): May 13, 1998	Active
AMSU B	NOAA-16 (NOAAL): Sep. 21, 2000	6/2014
MHS	NOAA-17 (NOAAM): Jun. 24, 2002	6/2002
	NOAA-18 (NOAAN): Aug. 30, 2005	Active
	MetOp-A: May 21, 2007	Active
	NOAA-19 (NOAAN'): Jun. 02, 2009	Active
	MetOp-B: September 17, 2012	Active
ATMS	NPP: October 28th, 2011	Active
	JPSS-1: 2017	N/A
	JPSS-2: 2022	N/A
	JPSS-3: 2026	N/A
TMI	Nov. 27, 1997	Apr, 2014
SSM/I	F-8: Jun. 20, 1987	Dec. 1991
	F-10: Dec. 1, 1990	Nov. 1997
	F-11: Nov. 28, 1991	May 2000
	F-13: Mar. 24, 1995	Nov. 2009
	F-14: Apr. 4, 1997	Aug. 2008
	F-15: Dec. 12, 1999	Active

*The AMSU A's and B's have flown together on the 3 NOAA KLM satellites. MHS replaces AMSU-B on NOAA-18 and 19.
**F-15: Beacon corrected data after Aug. 2006. – don't use for Climatology after this date

3.0 ALGORITHM DESCRIPTION

The GPM radiometer algorithm is based upon a Bayesian approach in which the GPM core satellite is used to create an *a-priori* database of observed cloud and precipitation profiles. Once a database of profiles and associated brightness temperatures is established, the retrieval employs a straightforward Bayesian inversion methodology. In this approach, the probability of a particular profile **R**, given $\mathbf{T_b}$ can be written as:

$$\Pr(\mathbf{R} \mid \mathbf{T_b}) = \Pr(\mathbf{R}) \times \Pr(\mathbf{T_b} \mid \mathbf{R}) , \quad (1)$$

where Pr(**R**) is the probability that a certain profile **R** will be observed and Pr($\mathbf{T_b} \mid \mathbf{R}$) is the probability of observing the brightness temperature vector, $\mathbf{T_b}$, given a particular rain profile **R**. The first term on the right hand side of Eqn. (1) is derived from the *a-priori* database of rain profiles established by the radar/radiometer observing systems discussed in section 3.1. The second term on the right hand side of Eqn. (1), is obtained from radiative transfer computations through the cloud model profiles. The formal solution to the above problem is presented in detail in Kummerow *et al*., (1996). In summary, the retrieval procedure can be said to compose a new hydrometeor profile by taking the weighted sum of structures in the cloud structure database that are radiometrically consistent with the observations. The weighting of each model profile in the compositing procedure is an exponential factor containing the mean square difference of the sensor observed brightness temperatures and a corresponding set of brightness temperatures obtained from radiative transfer calculations through the cloudy atmosphere represented by the model profile. In the Bayesian formulation, the retrieval solution is given by:

$$\hat{E}(R) = \sum_j R_j \frac{\exp\left\{-0.5\left(Tb_o - Tb_s(R_j)\right)^T (O+S)^{-1}\left(Tb_o - Tb_{s(R_j)}\right)\right\}}{\hat{A}} \quad (2)$$

Here, R_j is once again the vector of model profile values from the *a-priori* database model, Tb_o is the set of observed brightness temperatures, $Tb_s(x_j)$ is the corresponding set of brightness temperatures computed from the model profile R_j. The variables *O* and *S* are the observational and model error covariance matrices, respectively, and $\hat{A}$ is a normalization factor. The profile retrieval method is an integral version of the well-known minimum variance solution for obtaining an optimal estimate of geophysical parameters from available information (Lorenc, 1986, for a general discussion).

While the mechanics of Bayesian inversions are fairly well understood, four important issues are discussed separately in the following sections. The first concerns the use of ancillary data such

as Surface Temperature and Total Column Water Vapor (TCWV or TPW) to search only appropriate portions of the a-priori database. Previous studies such as Berg et al., (2006) have shown that searching only over the appropriate SST and TCWV over oceans constrains the solution in a significant and positive manner. An important step is, therefore, to select the appropriate *a-priori* profiles in the Bayesian inversion. In the current version of the algorithm, the a-priori database is sub-setted by 2-meter temperature (T2M), TCWV and Land Surface Classification For this search to work, the ancillary data must be added to both the retrieval as well as the a-priori database. It is therefore discussed first in section 3.1. The different sizes of passive microwave Field's of View (FOV) are discussed in Section 3.2. This section deals specifically with the issue of varying FOV sizes while retrieving a physical parameters which may be related to none of the channel spatial resolutions. The third is the construction of the *a-priori* database itself. Because the databases constructed for each constellation radiometer are based upon the output of the "combined radar/radiometer" algorithm in GPM, it must be noted that that product could not be used until after the launch of GPM and sufficient time afterwards to generate a robust database. As such, the at-launch algorithm utilized currently available hydrometeor observations from TRMM, CloudSat, and surface based radars to simulate GPM'S DPR radar. The next 2 post-launch versions (including this one GPROF2017 V1) used a combination of Combined product and Surface Radar observations to construct the a-priori database. The method of database construction of the GPM databases is detailed in section 3.3. The final section (3.4) then deals with the uncertainties that are assigned to each channel in the Bayesian retrieval framework.

3.1 ANCILLARY DATA

Ancillary data is attached to each of the observed pixels in the sensor preprocessors. These parameters are included computed to each database pixel, and observed pixel: Two Meter Temperature (T2M), Total Column Water Vapor (TCWV) , Surface Type, and Wet Bulb Temperature. Other parameters available, but not used for this version of GPROF are: surface skin temperature, lowest 500m temperature lapse rate, and a CAPE index. Also, to allow for future improvements in orographic precipitation, humidity and wind profiles are available. although they are not currently used. The source of ancillary data determines the output product type. Real-time data needed by the merged products (i.e. IMERGE) requires forecast model output to be available in near-real time (NRT) close to the time of satellite data collection. The Japanese operational GANAL product (in both forecast and analysis mode) is used for the "real-time" and "standard" products respectively, while ERA-Interim is be used for Climate Reference Product which requires homogeneous ancillary data over the climate time series. As described in section 4, this is handled in the sensor pre-processor portion of the algorithm to minimize changes to the retrieval code.

3.1.1 Creating the Surface Class Specification

The GPROF algorithm sub-sets the a-priori database by three different parameters: T2m, and TCWV (from model output) and 14 different surface classifications derived from a CSU surface classification scheme which intends to separate surfaces with similar microwave emissivity. Surface type classification begins with ten land classifications, ocean (or inland large water

bodies), sea-ice and the two different boundaries that are possible between the interfaces (land-ocean and ocean-sea ice).

To create the land surface classes Prigent *et al*. 1997, estimated land surface emissivities from all available SSM/I observations from 1993 to 2008, under clear sky conditions. The dataset has been extensively analyzed and evaluated, by comparisons with both related surface parameters and model outputs. It has been shown to provide robust emissivity calculations, *i.e*., radiative transfer simulations using the emissivities are closer to the satellite observations. These estimates of the emissivities for all SSM/I frequencies are available with a spatial resolution of 0.25°×0.25° at the equator (equal-area grid) at monthly averaged intervals.

The seven dimensional emissivity space of mean SSM/I emissivities have been clustered using a K-means or Kohonen method. The emissivity classes are static but are applied on a monthly basis so that a single point can change classes as a function of time. In Fig. 3, the globe is classified into 10 land classes for January (Prigent *et al*. 2008). In this example, classes 1 to 5 are for increasing vegetation cover classes, 6 to 9 are for increasing snow/ice-covered pixels, and class 10 is for inland water-covered pixels. The TELSEM tool was used to analyze the correlation structure and the covariance matrices for each class, and each pixel location.

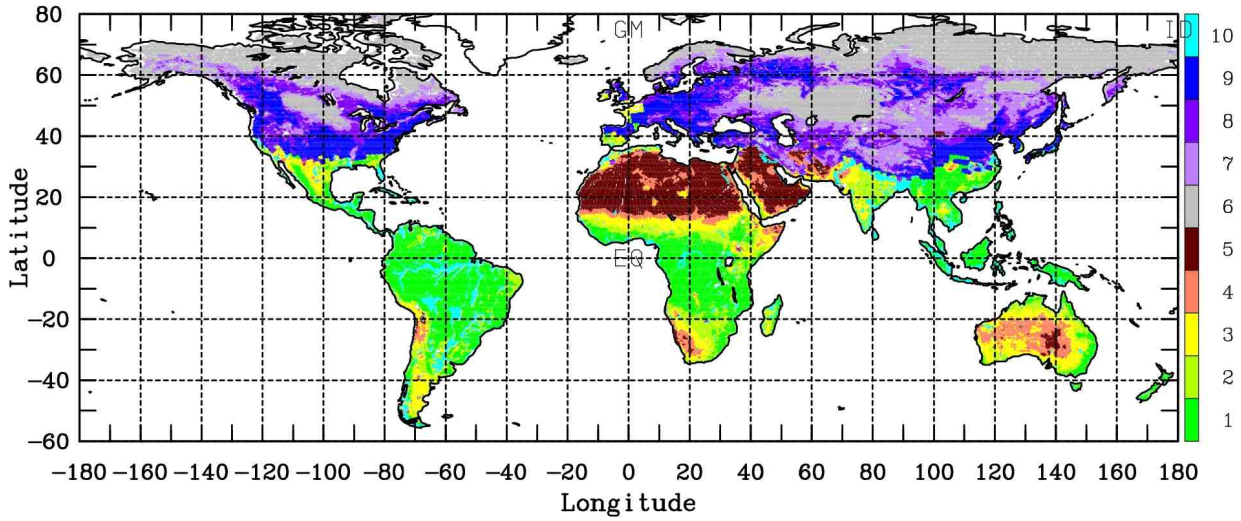

Fig. 3. Clustering of the SSM/I classes in ten self-similar emissivity classes. The ten classes have been defined corresponding to: five classes with increasing vegetation, four classes with increasing snow and ice and a class of what appears to be rivers/standing water/ estuaries.

For all versions of the GPM GPROF algorithm, the 10 land classes correspond to self-similar mean emissivities. Subsequent versions might use self-similar co-variances among channels. This change would better fit the GPM post-launch paradigm in that the combined GMI-DPR algorithm that would eventually replace the current algorithm would likely be based upon such a co-variance paradigm were the emissivities could be adjusted to achieve the optimal fit between GMI and DPR.

The Colorado State University Land surface definition is a sensor specific classification starting with these 10 surface classes. Then we define the GPM land/ocean boundary using a roughly

one km MODIS/SeaWIFS / Ocean Color land mask. This was initially generated in 1993 and based on the World Vector Shoreline (WVS) database. In October 1997, shortly after the SeaWiFS launch, the land mask database was modified to include inland waterways, based on the World Data Bank (WDB) information. The final result is a $1/128^{th}$ degree global grid that specifies either land or water. The GPROF sensor specific land mask files are on a $1/16^{th}$ degree grid, derived at the nominal sensor footprints of 19GHz.

In the GPROF classification, the above land mask defines 2 additional classes to add to the 10 land surface classifications: Ocean and large inland water, and Land/Ocean Boundaries (coast). The coast class is defined as the percentage of land falling within the 1/16th degree grid box to be between 2 and 95%.

Finally, the areas of sea-ice are defined from the NOAA Autosnow daily fields which have a 4 km resolution, available the day after real-time. The final CSU GPM surface classifications, and the ones output from the GPROF retrieval are numbered as:

1 : Ocean / Large inland Water
2 : Sea Ice
3 – 7 : Decreasing Vegetation Covered (3=Amazon, 7 = Sahara Desert)
8 – 11: Decreasing Snow Covered (8=Antarctica, 11 =lightly snow covered)
12 = : Inland Water / Rivers/ Estuaries
13 = : Coastlines (land/ocean boundary)
14 : Ocean / Sea-ice Boundary

In each of the GPROF sensor preprocessors, the daily land snow cover from the NOAA Autosnow product is used to update the daily snow cover to the current conditions.

3.1.2 Global Model Parameters

The JMA forecast model (JMA Fcst) is used for the GPROF near real-time (NRT) processing. Model data is assimilated every 6 hours for profile and surface parameters. Forecast global fields are available and used at the closest observation time, until the subsequent analysis is completed and transferred via the JMA to JAXA to PPS data flow.

For the GPROF Standard product (usually available within 36 hours of real-time) JMA Global ANALysis (GANAL) is used.

Retrieved surface parameters for both JMA FCST and GANAL are : surface pressure, MSL pressure, U and V component winds at 10 meters. 2 meter temperature. 2 meter relative humidity, and Skin Temperature. The vertical profiles on constant pressure surfaces are: Temperature, Vertical Velocity, U and V component winds, relative humidity, and geopotential height (the actual altitude of the pressure surfaces). The spatial resolution of the GANAL global grids is 0.5 X 0.5 degrees.

Approximately 2 months past real-time the ECMWF interim re-analyses are available. The

following data fields are downloaded and used for the GPROF2017 Climatological processing: 2 meter Temperature, 2 meter dew point, total column water vapor, surface pressure, and Skin Temperature. Also there are vertical profiles of Temperature, U and V component winds, specific humidity, and geopotential height (the actual altitude of the pressure surfaces). Model data is available every 6 hours for the profiles and 3 hours for the surface parameters. Spatial resolution is 0.75 X 0.75 degrees.

3.2 SPATIAL RESOLUTION

Observed microwave radiances generally do not have matched Field's of View. Instead, diffraction tends to limit the resolution of most channels. Spatial resolutions of GMI and constellation radiometers are listed in Appendix A. This creates a conundrum in that the spatial resolution of the retrieved precipitation cannot be linked directly to the resolution of the observations. Two solutions exist. The first is to leave all channels at their original resolution and simply define a separate spatial resolution at which hydrometeors are defined. Historically, either 19 or 37 GHz resolutions have been defined for the hydrometeors. The alternative is to convolve all brightness temperatures to a common spatial resolution and use it to define the hydrometeors. The code for doing this has been developed but not implemented. The resampling technique employed is that of Backus-Gilbert (BG) (1970) as applied to the TMI by Rapp *et al.* (2009). The BG technique uses the observed T_b's of the surrounding pixels to resample the observed T_b at a given scan position as a linear combination of those surrounding T_b's,

$$T_{BG} = \sum_{i=1}^{N} a_i T_{obs}(i),$$

where a_i are coefficients that must be computed for each channel and scan position. In this case an 11x11 array of surrounding T_b's are used for the resampling giving N=121. Because the antenna temperature measurement uncertainties are assumed to be uncorrelated, standard propagation of errors provides the variance in the deconvolved
T_b's as

$$e^2 = \left(\Delta T_{RMS}\right)^2 \sum_{1=1}^{N} a_i^2 \quad ,$$

where ΔT_{rms} is the uncertainty in the observed T_b's. Due to the potential for the propagation of large uncertainties, this technique requires a balance between resolution enhancement and amplification of noise. The details describing this process are provided in Rapp *et al.* (2009). Table 5 provides the uncertainty characteristics for the center pixel of the TMI swath for both the native resolution and the resampled resolutions. Particular care should be taken with the use of the T_b's resampled to the 37-GHz resolution, which has large uncertainties in the low frequency channels. Output files for TMI are available on an orbit-by orbit basis via anonymous ftp at rain.atmos.colostate.edu in directory /pub/GPM_Algorthm. The directory includes a simple program for reading the files as well as description of all data fields and formats. For GPM Version 5 of the algorithm, we continue to use the option using the original resolutions. However it appears that this may not have been properly implemented as the a-priori databases

were constructed assuming a common de-convolved resolution. Matched FOVs are planned for implementation in the next version - GPM V6.

Table 5. Noise values (e) in [K] at native resolution and computed for TMI T_b's resampled to the 19- and 37-GHz FOVs.

Frequency [GHz]	10.65	10.65	19.35	19.35	21.3	37.0	37.0	85.5	85.5
Polarization	V	H	V	H	V	V	H	V	H
e_{native} **[K]**	0.63	0.54	0.50	0.47	0.71	0.36	0.31	0.52	0.93
e_{19} **[K]**	1.61	1.59	0.50	0.47	0.47	0.12	0.11	0.09	0.16
e_{37} **[K]**	3.0	3.0	2.5	2.4	2.4	0.36	0.31	0.2	0.3

3.3 THE *A-PRIORI* DATABASES

The GPM V5 a-priori databases are constructed from one year (September 2014 – August 2015) of matched GMI/hydrometeor observations. One year is used to in order to capture the annual cycle of precipitation in the majority of meteorological conditions. For GPM V5, GMI radiances are matched with 3 hydrometeor sources- Combined MS, DPR Ku, and Multi-Radar/Multi-Sensor System (MRMS) ground-based radars.

First Source: The Combined MS product profiles of hydrometeors and surface precipitation derived from the DPR are used (parenthesis are GPROF surface types) over oceans (1), sea-ice(2), and sea-ice/ocean boundary(14).

Second Source: Version 4 of the Combined algorithm appeared to significantly overestimate precipitation over land. Therefore for V4 and also V5 the a-priori databases were constructed using DPR Ku surface precipitation for GPROF surfaces: vegetated (3-7), inland water (12), and coastlines (13). However, the Combined MS vertical hydrometeor profiles are still used for these surface types.

Third Source: Over land, the US based MRMS (ground-based radar) data was used to build a-priori databases for snow covered surfaces (8-11) for each of the constellations radiometers. Two years of MRMS data were matched up Tbs from each satellite sensor overpasses. This greatly improved the low bias that GPROF V4 had over snow covered surfaces. Because the MRMS data was only 2D and did not contain the vertical hydrometeor profiles, no vertical profile information is available from the GPROF retrieval over snow covered surfaces.

GPROF for GPM V5 uses the previous version (i.e. V4) of the Combined and DPR-Ku products for its databases. Future versions of GPROF, because of its need for existing GPM products to construct it's a-priori database, will always be one version behind the Combined algorithm. In GPROF for GPM V5, we nonetheless improved some of the ice hydrometeor simulations in order to get better agreement between computed and simulated brightness temperatures. This leads to smaller bias adjustments in the radiometer simulations and leads to an overall better fit

between the radiometer retrievals and both the Combined products as well as ground validation data.

Examination of the database simulations using the initial ice amounts and spherical ice particles from the V4 Combined DPR/GMI Algorithm product suggested that, though successful in matching observed Tbs at frequencies of 89 GHz and below, it was not possible to obtain agreement in a multi-specular way at the higher frequencies using the spherical particles. The ice was therefore adjusted as follows: ice contents from 2BCMB are used in the database simulations as a first guess. Ice particles are assumed to be non-spherical, and are represented as an ensemble of particle shapes, with single scatter parameters derived from the database produced at Florida State and described in Liu 2008. A simple exponential PSD is used to calculate the bulk optical properties. Resulting Tbs are then compared to GMI observations and adjusted iteratively to optimize agreement at 166 GHz. Residual high-biased disagreement at 183 GHz +/-3 is additionally improved by the addition of small cloud ice particles.

This adjustment process is designed to decrease simulation biases in the higher frequency channels. It is anticipated that in future versions of the algorithm, such adjustments will be unnecessary as the 2BCMB product begins to utilize the more realistic non-spherical ice particles within the DPR/GMI retrieval system starting with version 5.

GPROF for GPM V5 also made additional changes to retrievals of high latitude oceanic drizzle and snowfall over land. Both these changes were made because the DPR sensitivity of 12 dBZ was shown to miss substantial amounts of drizzle and light to moderate snowfall events. Because the GPM radars do not have signal in these cases, they are not addressed in the newer versions of the Combined and Radar products either. Drizzle was addressed in the a-priori database by setting a threshold in the cloud liquid water retrieval from GMI (done before the DPR or Combined rainfall is inserted into the scene), to match the CloudSat based probability of rainfall. This is done for each temperature and Total Column Water Vapor (TCWV) bin used to subset the a-priori database. While this assumes that higher cloud liquid water amounts correspond to precipitation, the assumption is generally thought to be reasonable. Additional cloud water beyond the CloudSat determined threshold was partitioned between Cloud- and rain water similar to the procedure used by Hilburn and Wentz (2008). This increases rain water at high altitudes to agree better with CloudSat and ERA and MERRA re-analyses but continues to be low relative to these estimates. More work in ongoing to assess high latitude drizzle from different sources.

Some construction facts about the database:

- There are approximately 400 million matched GMI / Surface precip profiles from all sources
- Combined MS database was for September 2014 – August 2015 uses only the middle 21 pixels
- For MRMS matchups over the US, 2 winters were used, April 2014 – May 2016.
- The a-priori database is subsetted by : 0-78mm TCWV, 220 – 320 T2m, and 14 surface types
- Tbs are at their native resolution
- ECMWF, and GANAL databases are used for defining pixels TCWV, and T2m, and Surface Wet Bulb Temperature

- CSU created surface maps are for 14 surface types

3.3.1 Matching Sensor Tbs to the Database Profiles

The first step in the a-priori database construction is to use the DPR surface precipitation and layered hydrometer profiles in a forward model radiative transfer calculation to compute satellite radiances for the Tb frequency sets of GMI, SSMIS, TMI, AMSR-2, and the cross-track radiometers, MHS, ATMS, and SAPHIR. The DPR liquid and ice water content profiles are calculated for 28 vertical levels using the 2A25 Z-M relationship coefficients and the 2A25 freezing level information. Surface rain rate is also included, and the observed TMI brightness temperatures at each frequency and polarization. The PR hydrometeors are then averaged into the 22GHz footprint using the nominal cross-track and down-track resolution for each sensor while the Tbs are kept at their native resolution. There are approximately 290 million DPR profiles used in the time period : September 2014 – August 2015.

3.3.2 Ancillary Data Added to the Profile Pixel

The next step uses the time and location of each DPR pixel to add 'ancillary' data to the pixel. These are added parameters necessary to group the pixels by common meteorological, and surface emissivity conditions. Depending on whether the database is to be used for the GPROF near-real time, Standard, or Climatology products, data from the GANAL or ECMWF ERA-Interim model output is added to each footprint averaged DPR pixel. These parameters include two-meter surface Temperature (T2m) and Total Column Water Vapor (TCWV) and a calculated surface web bulb temperature. Interpolation of the model is then performed to an hourly resolution and smoothing to 0.25 degrees using a boxcar averaging. This greatly helps in eliminating ECMWF and GANAL model artifacts from the final precipitation products. The CSU defined surface type is then also attached to the pixel. At this time the Path Variables (Cloud Water, Rain Water, and Ice) are calculated from the DPR profiles. Once again we state: because the MRMS data was only 2D and did not contain the vertical hydrometeor profiles, no path information is available from the GPROF retrieval over snow covered surfaces. Also, here the surface precipitation amounts less than 0.01 mm/hr are set to zero.

3.3.3 Final Clustering of Binned Profiles

For each T2m/TCWV/Surface bin a clustering routine was used to decrease the number of profiles. A maximum of 800 profiles were kept along with a frequency of occurrence of the profiles within a given cluster (for each TCWV / T2m sorting bin). The clustering broadens the TCWV range up to +/- 4 mm. This has the intended effect of smoothing the profiles in the each clustered bin, and also increasing the total number of profiles in each bin. The TCWV broadening happens gradually until a maximum of 300,000 profiles is included in each of the 800 profile clusters within the bin. The final individual sensor GPROF database is made of 14 files, one for each surface type. GPROF2017 uses these 14 files to run the final the Bayesian rainfall retrieval.

3.3.4 Databases for Cross-Track Scanners

The process for creating the databases for the Cross-Track sounding instruments, MHS and ATMS are very similar, however there are some major differences. The conical imager radiometers have a constant Earth Incident Angle (EIA) defined as the pointing angle of the instrument towards the earth's surface. Therefore, when running the forward model radiative transfer, only a single EIA needs to be included for the path through the atmosphere. However, the cross-track instruments have a variable EIA with each of the 90 scan positions. To most accurately calculate the top of the atmosphere Tbs, the forward model would need to run using the EIA of each of the scan positions, but this isn't feasible in either processing time, nor in implementation of the operational GPROF retrieval. Tests were performed to determine the minimum number of angles necessary to stay within 1K error from a full 90 scan RT. Since the radiometers are symmetric on each side of NADIR, there are then only 45 scan positions to retrieve. We found that using 3 scan angles, would optimize the processing time and stay within the required RT error. In addition, we run the RT on +/- one scan position from the 3 defined angles to calculate a delta Tb/scan position variable. This is passed through to the GPROF retrieval so that the database Tbs can be adjusted on the fly to match exactly the Tbs that are expected from the Satellite Observed Tbs.

This is not perfect for many reasons, but Fig 4 shows the effect on the GPROF retrieval using the 3 angle databases (5 total over both sides of the scan), with and without the scan position Tb correction. The orange line shows the remaining cross-track bias in the rain retrieval. For each of the 14 surface classes, 3 databases corresponding to the three EIAs are created. Therefore, the GPROF2017 V1 retrieval reads in 42 unique databases filled with clustered profiles for the each of the TCWV/T2m profile bins.

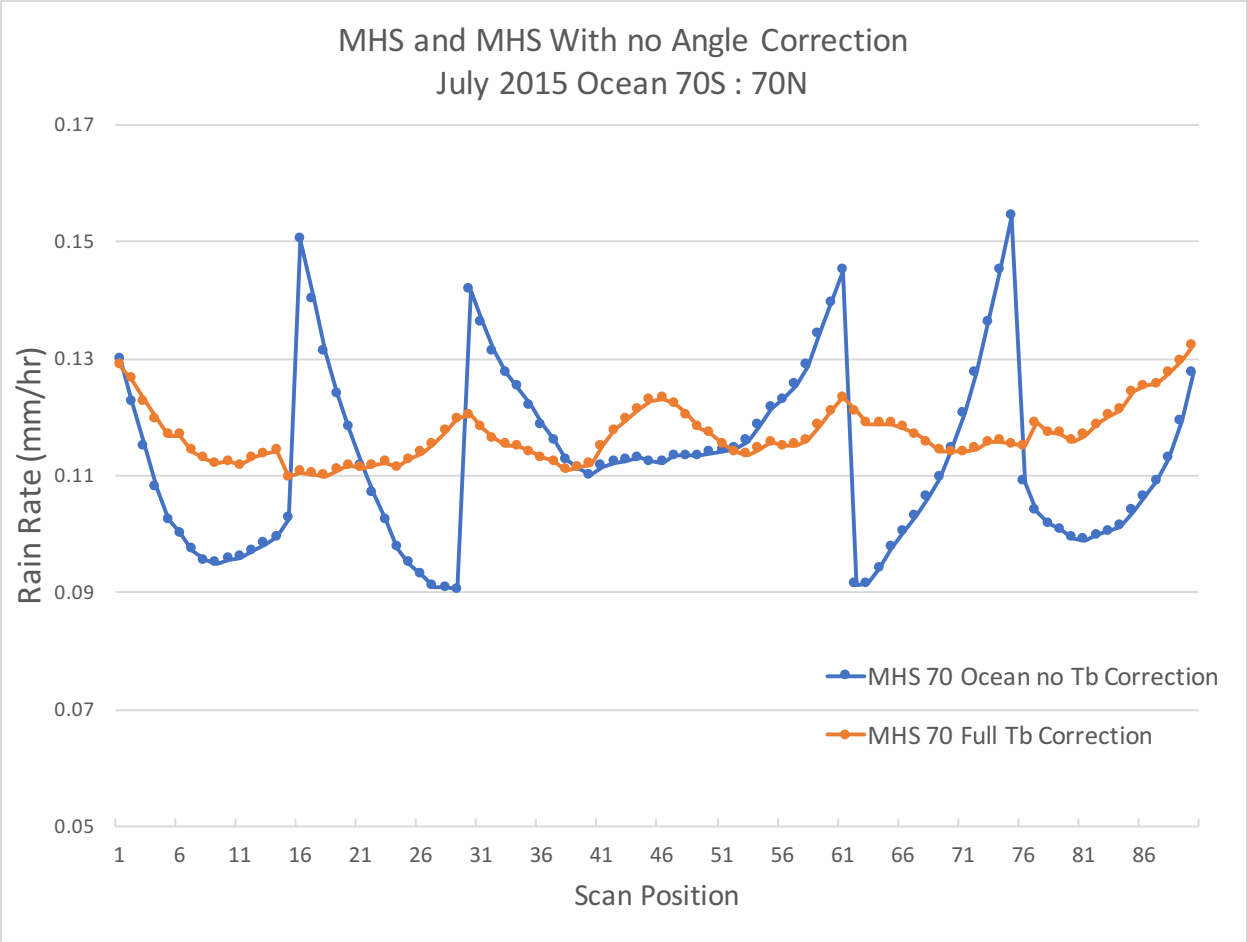

Figure 4. Scan position bias of rain rate for MHS using 3 unique databases. Blue line is without Tb Scan position correction, orange line is the final MHS retrieval including Tb scan position correction.

3.4 CHANNELS AND CHANNEL UNCERTAINTIES

Uncertainties in physical inversions come from a combination of sensor noise and forward assumptions and errors. As described in Stephens and Kummerow (2010), rainfall retrieval errors tend to be dominated by the forward model assumptions. That is the case here as well and is particularly true when surface characteristics are not well known

In the GPROF 2017 V1 retrieval, the uncertainty is determined from the fit between the observed dataset and the CRM T_b that ultimately make the a-priori database. But there are modifications to this simplistic approach primarily due to foot print size based on the number of DPR pixels averaged into the sensors 22 GHz footprint. For SSMIS which has a footprint 4 times GMI, the channel error used in the retrieval is approximately ¼ of GMI. Also for the cross-track sensors, we've found that as the footprint gets larger with distance from NADIR, the channel sensitivity

values must decrease to match the rain rates across the scan. A smooth reduction of the Channel Sensitivity values from the middle of the scan out to the edge- of-scan, are included in the cross-track GPROF Bayesian retrieval.

3.5 PRECIPITATION PROBABILITY THRESHOLD

New in GPROF 2017 V1 (GPM V5) is the application of a probability of precipitation (POP) directly to retrieved precipitation values. The POP thresholds for rain/no-rain are calculated for each sensor, are bin (TCWV/T2m/Surface class) dependent, and are calculated as described below.

For each of the bins in the database the number raining and non-raining profiles are calculated. Precipitation above the 0.01 mm/hr threshold is counted as raining and below to non-raining. This rain fraction ratio for each bin is calculated and stored. As example is that in warm/moist bins the rain/(rain+norain) ratio is near 0.70 (70%) while in cooler dryer climates it might be 0.05 (5%). We then create a year of GPROF rain retrieval and without any probability thresholds applied. From that year of retrievals, we collate the frequency of rain, and a histogram of POP for each bin. We then calculate the needed POP threshold that matched the database rain frequency, and set a POP threshold for that bin. Finally, we compute the fraction of rain that is removed using this POP threshold. The POP threshold, and the fractional rain that is removed by the threshold is output and saved in a file that's read into the GPROF retrieval.

During the GPROF retrieval process, precipitation with probability below the threshold is set to 0.0. Retrieved Precipitation about the threshold is increased by the fraction of removed precipitation. This method conserves the total precipitation of the retrieval, an important step in the Bayesian statistical scheme.

3.6 PRECIPITATION TYPE (Liquid vs. Frozen) DETERMINATION

The GPROF Bayesian retrieval which matches the satellite radiances with hydrometeors from the 3 input sources retrieves the total surface precipitation, not the phase of the precipitation. An additional piece of information is needed to categorize the retrieval as raining or snowing - the surface dew point temperature. From (Sims and Liu, 2015) we use a lookup table of the fractional precipitation that is liquid at certain dew point temperatures. At -6.5 ^{o}C and below, 100% of the precipitation is frozen, while above 6.5 ^{o}C the precipitation is all liquid. Between these extremes, the precipitation is mixed and each type is output in the GPROF output file. There are 2 different lookup tables, one for ocean and one for land. The look tables which use the surface wet bulb temperature and used in GPROF are graphically described in Fig. 5.

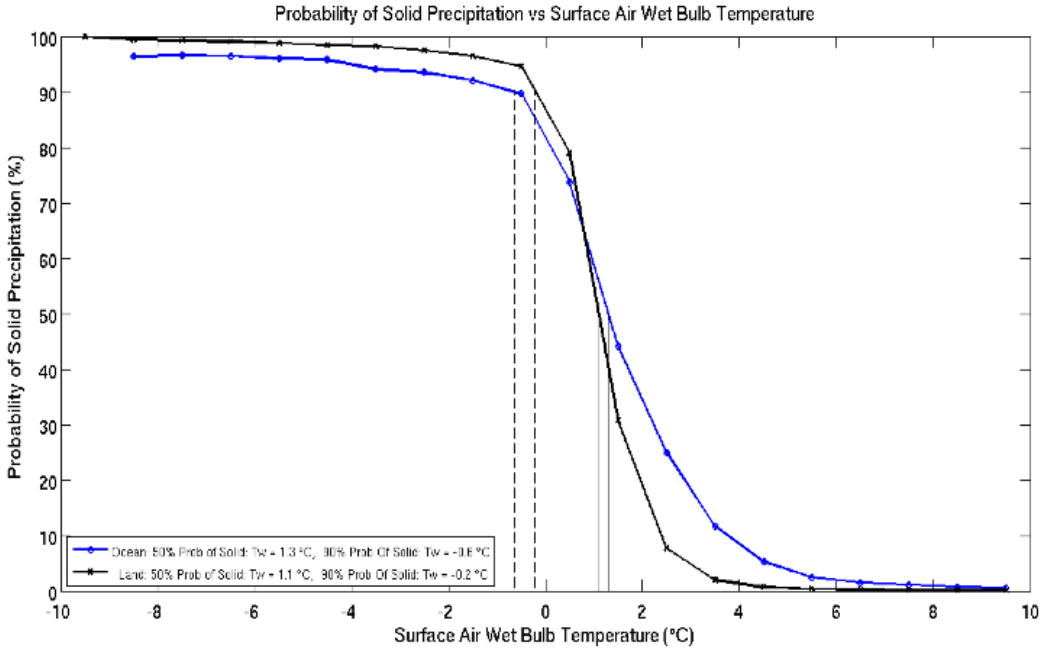

Figure 5. Solid Vs. Liquid Precipitation and Wet Bulb (Sims and Liu, 2015). Ocean is in blue, land in black.

4.0 ALGORITHM INFRASTRUCTURE

The code to ingest T_bs and ancillary files, perform quality control, assign surface types and decide on channel selection is written and maintained at Colorado State University in Fort Collins, Colorado, USA. The architecture is open to all team members as well as outside parties. We will use the input and output sections of this ATBD as a living document that is intended not only for the user of the precipitation product, but also for the algorithm developers to convey precise information about procedures, methods and formats. The code strives to be machine independent but will first order everyone on the algorithm development team to match the architecture planned by the PPS.

The algorithm itself consists of Fortran 90 code that's self-contained in the GPROF_2017_V1 algorithm directory. All parameter fields and static databases must be accessible from this directory location as well as the dynamic ancillary data fields.

4.1 ALGORITHM INPUT

The algorithm requires Level 1C brightness temperatures from each sensor, as well as accurate location of the sensor. In additional many 'ancillary' parameters are added that are required by the GPROF retrieval. These include individual sensor land masks, NOAA's Autosnow, and land surface classification, to create the daily surface classification. There are also the JMA Forecast, GANAL, or ECWMF daily model global grids used.

4.2 PROCESSING OUTLINE

Four processes are run at the PPS to complete the GPROF Precipitation Algorithm. The following sections present a short description of each, and graphically represented in the Fig. 6.

4.2.1 Model Preparation

The model preparation process ingests the JMA Forecast, GANAL and ECMWF GRIB formatted files. The files are unpacked into simple binary grids and any additional parameters needed by the preprocessor (e.g. GANAL TCWV from a profile of relative humidity, and surface wet bulb temperature are computed. Other data processing space and time interpolation between the 6 hourly model times to up to hourly fields. Output is to a multi-parameter structure of all variables needed by GPROF2017 V1 at each model grid point. This model prep routine can be modified easily for additional parameters that might be specified in the future. Modelprep is run each time a new model field is transferred to the PPS, and the files are stored.

4.2.2 Preprocessor

The preprocessor is the interface between the orbital data files (L1C format) and the GPROF2017. The GPM sensor specific preprocessors read from the L1C HDF files and create the standard input file format. The preprocessor assigns all the ancillary data to each observed pixel along with the pixel's T_{bs}, latitude/longitudes, and sensor specifications. Also here in the preprocessor, the emissivity class, land masks, sea-ice, and model surface 2-meter temperature are used to create a surface classification for each pixel. Other parameters are output including the names and locations of the ancillary data directories, and profile databases - everything the GPROF 2017 needs to run the rainfall retrievals. A description of the output parameters of the preprocessor is given in Section 4.3.

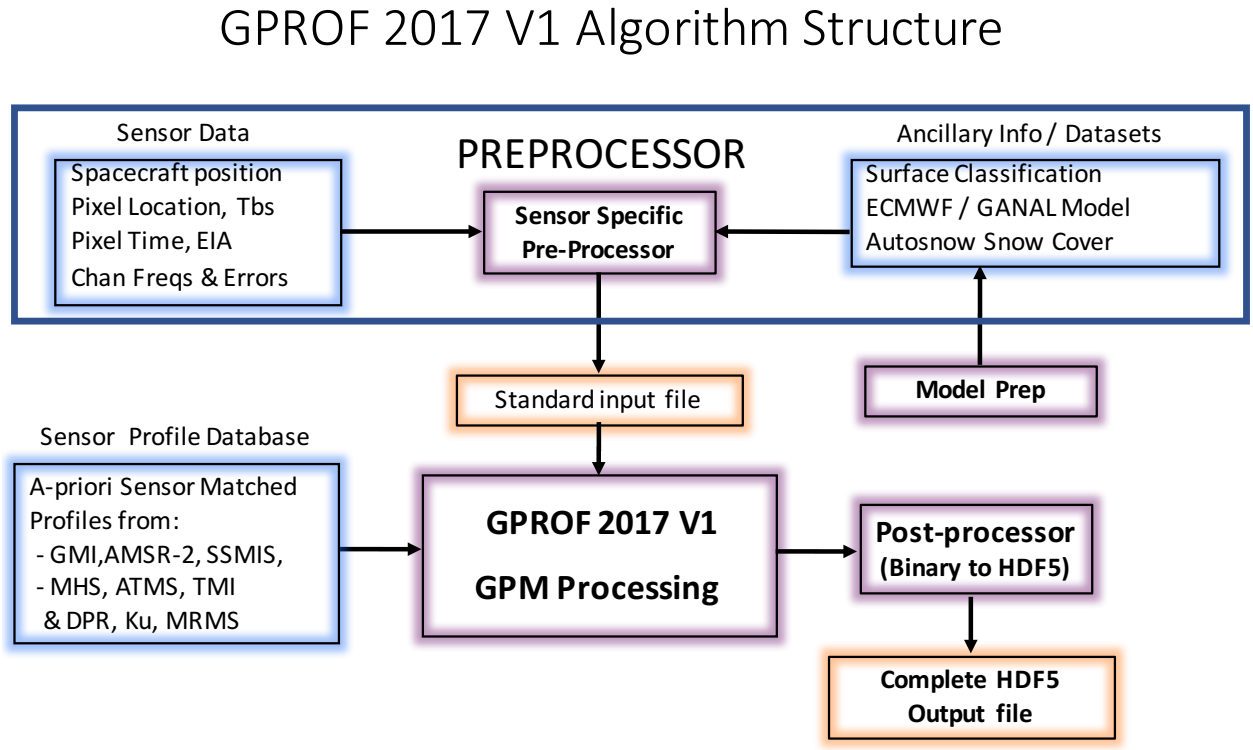

Figure 6. Overview of the processing concepts for the GPM Processing Algorithm.

4.2.3 GPM Rainfall Processing Algorithm - GPROF2017

GPROF 2017 starts by reading the Standard Input file produced from the preprocessor. This includes all the ancillary data needed to match the T2m/TCWV/SurfaceType in the profile databases. This 3-dimensional matching is used to subset the entire set of database profiles for the Bayesian precipitation and profile retrieval. The width of the search in T2m/TCWV space is variable in TCWV space in the database creation depending on the number of binned profiles, in the retrieval +/- 1 K is used in the T2m bin space. All the conical imager sensors use the identical GPROF 2017 V1 code.

If the 'run vertical profile flag' is set when GPROF executes, then the vertical profiles of the hydrometeor species are created. These are matched to the closest profile from a database of 960 representative profiles for each species. This step reduces the data volume of the output files. The output is to a native binary formatted file, and a description of the output parameters from the GPM PA is given in Section 4.4.

The cross-track sensors have a different executable : GPROF 2017 V1x. The only differences are the number of sensor channels (5 instead of 15), and the number of databases read in. There are the same 14 surface class databases, but for each of the 3 vie angle databases for a total of 42.

4.2.4 GPM Post-Processor

The GPM Post-processor reads the CSU native binary output and attaches additional metadata from the original orbital L1C file and writes out a final formatted HDF5 formatted GPM V5 - GPROF2017 file.

4.3 PREPROCESSOR OUTPUT

4.3.1 Preprocessor Orbit Header

satellite	Character*12	
sensor	Character*12	
preprocessor version	Character*12	
original radiometer file	Character*128	
profile database file	Character*128	
calibration file	Character*128	
granule number	integer*4	
number of scans	integer*4	
number of pixels in scan	integer*4	
number of channels with data	integer*4	
channel frequencies	real(15)*4	or real(5)*4 for MHS and ATMS
comment	Character*40	

note : channel_freq describes the exact frequencies of the channels, but they must be in the following order: 10v, 10h, 19v, 19h, 23v, 23h, 37v, 37h, 89v, 89h, 166v, 166h, 183_1v, 183_3v, 183_7v

4.3.2 Preprocessor Scan Header

ScanDate (6)	integer(6)*2	: year,month,day,hour,min,sec
Spacecraft latitude	real*4	
Spacecraft longitude	real*4	
Spacecraft altitude	real*4	

4.3.3 Preprocessor Data Record

Latitude	real*4	
Longitude	real*4	
Brightness temperatures	real(15)*4	real(5)*4 for MHS, ATMS
Earth Incident angles	real(15)*4	real*4 for MHS, ATMS
Wet Bulb Temperature	real*4	
Lapse Rate	real*4	
Total Column Water Vapor	real*4	

Skin temperature		real*4	
2 Meter temperature		real*4	
L1C quality Flag		integer*4	
Sunglint angle	I	integer*1	
Surface type code		integer*1	
CAPE index		integer*2	Always set to missing for GPROF 2017 V1

4.4 GPM PRECIPITATION ALGORITHM OUTPUT

Whether in the native, HDF formats, the output parameters will be equivalent. This following format description is for the GPM native output binary format file.

4.4.1 Orbit Header (at beginning of each file) (described in section 4.4.5)

Satellite	Character*12	
Sensor	Character*12	
Pre-processor Version	Character*12	
Algorithm Version	Character*12	
Profile Database Filename	Character*128	
Original Radiometer Filename	Character*128	
File Creation Date/Time(6)	integer*2	
Granule Start Date/Time(6)	integer*2	
Granule End Date/Time(6)	integer*2	
Granule Number	integer*4	
Number of Scans in Granule	integer*2	
Number of Pixels/Scan	integer*2	
Profile Structure Flag	integer*1	(0=no, 1 = yes)
Spares	51 bytes	

4.4.2 Vertical Profile Structure of the Hydrometeors (described in section 4.4.6)

Profile database partitioned by species and 2 meter air temperature. Nominally, there are 2100 possible unique profiles for each species, each with a general scale factor.

Number of Profile Species - Nspecies	integer*1	(5, defined in Species Description)
Number of Profile Temps - Ntemps	integer*1	(12, defined in Temp Description)
Number of Profiles Layers - Nlyrs	integer*1	(28, defined in HgtTopLayer)
Number of Clustered Profiles – Nprfs	integer*1	(80)
Species Description(Nspecies)	character*12*5	
Height, Top of Layers(Nlyrs)	integer*2	
Temperature Descriptions(Ntemps)	real*4	
Cluster Profiles(Nspecies,Ntemps,Nlyrs,Nprf)	real*4	

4.4.3 Scan Header (at beginning of each scan, described in section 4.4.7)

Spacecraft latitude	real*4
Spacecraft longitude	real*4
Spacecraft altitude (km)	real*4
Scan Date/Time (yr,mon,day,hour,min,sec,millisec)	integer*2
Spares	integer*2

4.4.4 Pixel Data (for each pixel in scan, described in section 4.4.8)

Pixel Status	integer*1	(one byte)
Quality Flag	integer*1	
L1C Quality Flag	integer*1	
Surface Type Index	integer*1	
Total Col Water Vapor Index	integer*1	
Probability of Precip	integer*1	
2-meter Temperature	integer*2	
CAPE	integer*2	
Sunglint Angle	integer*1	
Spare	integer*1	
Latitude	real*4	
Longitude	real*4	
Surface Precipitation	real*4	
Frozen Precipitation	real*4	
Convective Precipitation	real*4	
Rain Water Path	real*4	
Cloud Water Path	real*4	
Ice Water Path	real*4	
Most Likely Precipitation	real*4	
Precip 1st Tertial	real*4	
Precip 2nd Tertial	real*4	
ProfileTemp2mIndex	integer*2	
Profile Number(5)	integer*2	
Profile Scale(5)	real*4	

4.4.5 Orbit Header Variable Description – total of 400 bytes

Satellite

Generally this is a character string for the satellite which produced the data. For example: GPM, MeghaTropics, DMSP-F10, TRMM, WNDSat

Sensor

Satellite Sensor, currently:
GPI, MAD, AMSR-E, SSM/I, SSMIS, TMI, WINDSAT, and others

PreProcessor Version

GPM Pre-Processor version number.

Algorithm Version

GPM Processing Algorithm Version which produced the output file.

Profile Database Filename

File name of the profile database. May be expanded to include multiple databases.

Original Radiometer Filename

File Name of the original, satellite observation input data file.

File Creation Date/Time

Start date and time of file creation. Defined as the date/time structure which holds six integer*2 values - year, month, day, hour, minute, second.

Granule Start Date/Time, End Date/Time

Start and End dates and times of first and last scan in file. Defined as the date/time structure, which holds year, month, day, hour, minute, second.

Granule Number

Generally this is defined as the satellite orbit number since launch.

Number of Scans in Granule, Number of Pixels per Scan

Number of sensor scans in the file, Number of pixels per scan for this sensor

Profile Structure Flag

Flag defining whether GPM Profiling Algorithm was run with vertical profiles of the hydrometeors. No structure = 0, with vertical structure = 1.

Spares

51 spare bytes for additional parameters.

4.4.6 Vertical Profile Variable Descriptions

These variables are always included even when the hydrometeor profiles are not computed. In this case the values will be set to missing. Section 4.6 describes the recovery of the retrieved hydrometeors profile using these profile variables.

Number of Profile Species

The number of different species (5). The character description of each is in the Species Description Variable below.

Number of Profile Temps

The number of profile temperature indices (12). The exact values of the indices are given in the Temperature Description Variable below.

Number of Profiles Layers

Defined for GPM profiling algorithm as 28.

Number of Clustered Profiles

Number of unique profiles for each species and 2 meter Temperature index (80, nominally)

Species Description

Nspecies (5) number of character descriptions of Species, e.g. "Cloud Water Content"

Hgt Top Layer

Height of the top of each 28 layers of GPM PA in kilometers (km). These are defined every 0.5 km up to 10 km, then every kilometer after that up to 18 km. Values are: 0.5, 1., 1.5, 2., 2.5, 3., 3.5,4.,4.5,5.,5.5, 6.,6.5,7., 7.5, 8., 8.5, 9., 9.5,10., 11., 12., 13., 14.,15., 16., 17., 18.

Temperature Descriptions

Values of Ntemps number of 2m temperature indexes, these values are:
270, 273, 276, 279, 282, 288, 291, 294, 297, 300, 303

Cluster Profile Array

The array which holds the standard GPM profile structures.

4.4.7 Scan Variable Descriptions

Spacecraft latitude, Spacecraft longitude, Spacecraft altitude (km)

Satellite sub-point earth coordinate position and altitude

Scan Date/Time (7)

Time at the beginning of the scan including milliseconds. (Year, month, day, hour, min, sec, millisecs.

4.4.8 Pixel Data Variable Descriptions

Pixel Status – a full list of these can only be created once the algorithm is finalized.

If there is no retrieval at a given pixel, pixelStatus explains the reason.

0 : Valid pixel
1 : Pixel out of Latitude/Longitude defined area
2 : Tbs out of range
3: Surface code / histogram mismatch
4: Missing tcwv,T2m, surface code from the preprocessor
5: no Bayesian solution possible

Quality Flag

The GPROF Quality Flag variable for GPM V5 has added one additional index. The old indices in V3 and V4 included values: 0,1,2. The new index can be 0,1,2,3

Value 0: pixel is "good" and has the highest confidence of the best retrieval.

Value 1: "use with caution" . Pixels can be set to value 1 for the following reasons:

5) Sunglint is present, RFI, geolocate, warm load or other L1C 'positive value" quality warning flags
6) All sea-ice covered surfaces
7) All snow covered surfaces
8) Sensor channels are missing, but not critical ones.

Value 2: "use pixel with extreme care over snow covered surface" This is a special value for snow covered surfaces only. The pixel is set to 2 if the probability of precipitation is of poor quality or indeterminate. Use these pixels for climatological averaging of precipitation, but not for individual storm scale daily cases.

Value 3: "Use with extreme caution". Pixels are set to value 3 if they have channels missing critical to the retrieval, but the choice has been made to continue the retrieval for these pixels.

L1C Quality Flag

Within the Preprocessor, checks are made of the L1C quality flag. These quality flags have both fatal error and non-fatal warnings. These are checks and a new code 0,1,3 is passed through to GPROF. Generally:

0 = do retrieval
1 = some problems, or channels are missing
3 = retrieval has many channels missing and probably shouldn't be used.

If the L1C quality flag have a fatal error, the pixel's Tbs are set to missing.

Surface Type Index

Surface type codes are: 1 : Ocean, 2 : Sea ice, 3-7 : Decreasing vegetation, 8-11 : decreasing snow cover, 12: standing water, 13 : land/ocean or water coast, 14 : sea-ice edge

Total Column Water Vapor Index

The integer of the model total precipitable water (mm) used to select the correct database profiles. It's the nearest integer of the actual real*4 Model output value.

Probability of Precipitation

A diagnostic variable, in percent, defining the fraction of raining vs. non-raining Database profiles that make up the final solution. Values range from 0 to 100%.

2 Meter Temperature Index

The integer value of the model 2 meter temperature -used to select the correct database profiles. It's the nearest integer of the actual real*4 Model output value.

CAPE

Available Convective Energy Parameter. All values set to missing, it's not used in GPROF 2017 V1. This will be used in later versions of GPROF when separating convective and stratiform profiles.

Sun Glint Angle

Conceptually, the angle between the sun and the instrument view direction as reflected off the Earth's surface. sunGlintAngle is the angular separation between the reflected satellite view vector and the sun vector. When sunGlintAngle is zero, the instrument views the center of the specular (mirror-like) sun reflection. Values range from 0 to 180 degrees. If this angle is < 10 degrees, the pixel is affected by sunglint and the pixels Quality Flag is lowered.

Latitude, Longitude

Pixel latitude and longitude.

Surface Precipitation

The instantaneous precipitation rate at the surface. Check pixelStatus for a valid retrieval. Values are in mm/hr.

Frozen Precipitation, and Convective Precipitation

The instantaneous frozen and convective precipitation at the surface. Values are in mm/hr.

Rain Water Path, Cloud Water Path, Mixed Water Path, and Ice Water Path

Total integrated rain water, cloud liquid water, mixed phase water and ice water in the vertical atmospheric column.

Most Likely Precipitation

The surface precipitation value (mm/hr) with the highest occurrence within the Bayesian retrieval.

Precipitation 1st Tertial and 2nd Tertial

The surface precipitation value (mm/hr) at the 1st and 2nd tertiary of the precipitation distribution.

Profile Indexes: ProfileTemp2mIndex, ProfileNumber, ProfileScale

Profile Scale (one for each hydrometeor species), Profile Number, and Profile 2 meter temperature index, used as a reference into the corresponding cluster profile array. These define the correct hydrometeors profile for each pixel. The retrieval of the profile using these values is described in section 4.5.

4.5 HYDROMETEOR PROFILE RECOVERY

In order to recover hydrometer profile values of a single pixel, use the profileNumber, profileScale and 2mTempindex parameters, select your species and loop over the levels by plugging these indices into the 'clusterprofile' array. Where:

S = species(1-4) 1 = cloud water content
2 = rain water content
3 = mixed water content
4 = ice water content

T = 2 meter temp index
L = profile level (1-28). The top of each level is specified in HgtTopLayer
P = profileNumber

Pixel value = ProfileScale(S) * clusterprofile(S,T,L,P)

4.6 HISTORICAL RECORD : THE PRE-LAUNCH ALGORITHM

This section is a historical record of GPM planning. It is included simply for completeness of the GPM GPROF project.

The algorithm, being Bayesian, need *a-priori* databases reflecting the true state of the atmosphere. Before the launch of GPM, this database was constructed from various sources. Its construction is separated into components.

PI Profiles. These are individually observed or simulated hydrometeor profiles and corresponding T_{bs} delivered by PIs on the algorithm team. PIs are asked to deliver the surface rainfall, hydrometeor vertical profiles and corresponding T_b at the original sensor resolution as well as a TMI/AMSR-E 37-GHz resolution. Details of the fields are found in Appendix B.

Observed profiles' datasets that have been discussed to date:

Name	Region	Contact	Status
PR +TMI/satSensor	Tropics	Sarah Ringerud	V1 completed

CloudSat/AMSR/MHS	Ocean + Land(snow)	Mark Kulie	V1 completed
NMQ/ SatSensors	CONUS	Veljko Petkovic	V1 completed

Immediately after launch, an empirical database could be created using the DPR surface rain and hydrometeor profiles together with the observed GMI T_b convolved to resolutions of the other conical sensors. However to replace the surrogate a-priori databases at least of year of GMI/DPR observations are necessary

Sounding radiometers are fundamentally different in that neither PR/TMI nor CloudSat/AMSRE/MHS, can be used to create observed databases. Instead, we rely on coincident overpasses and the model derived databases.

PR + TMI Coincidence	Land and ocean – 40N : 40S
NMQ + SSMIS	Conus
CloudSat/AMSR-E/MHS	global, poleward of 30 degrees

After the GPM launch, we will likely continue to use the model-based profiles, which will be enhanced through coincident overpasses between the GPM core satellite and available sounding radiometers. This will give us time until the "Combined" product is sufficiently mature to produce the physical databases needed to have confidence in the simulated T_b for the sounding radiometers.

PI profiles were collected, enhanced with ancillary data from GANAL/ECMWF, and binned according to surface temperature, total precipitable water, and surface classification (currently 15 classes, 10 defined by Felipe Aires as self-similar emissivities + sea-ice + 3 coastal classes). The current set of ancillary parameters is listed in Appendix B. The PI profiles with common format and ancillary data are referred to as binned GPROF databases. (Note: The MMF based profiles may need to add some of their own ancillary variables insofar if ECMWF fields are not appropriate for these simulations.)

The above databases are quite large – reaching up to millions of profiles in a given bin. For GPROF 2014 to run, one needs to cluster these entries to be efficient as was done in GPROF2010. While clustering changes the final retrieval result only slightly, the step is cumbersome and not ideal for research purposes (*i.e.*, every time you try something new you have to go through a large clustering procedure before the algorithm can be run). Because of that, GPROF 2014 will have a research and an operational version. The research version will work on a single surface temperature, TCWV, and Surface type. It runs successively over multiple bins but is rather slow – 30-60 minutes per orbit. The benefit is that the algorithm is easy to modify by all PIs for research purposes. The operational version will be created from the best research results and only when needed for testing by the PPS. Version B2, which this document describes is the science version of the algorithm.

The retrieval, as discussed at the GPM Algorithm Working Group Meeting in July 2011, has three variants to reflect that we either know nothing about the surface emissivity (S0), we know something about the surface emissivity (S1) or we have a Land Surface Model (LSM) to predict

the key emissivity parameters (S2). Aside from using it in the retrieval, this LWM will have to be run for the period covering the databases. Specifically, the LSM variables would be added to all appropriate profiles in the same step as the other ancillary data is added to the hydrometeor profiles and T_b.

If we know nothing about the surface, we will run the algorithm variant that Grant Petty proposed that uses channels that effectively get rid of the surface variability. Call this a S0 (for Surface 0) retrieval. It looks at only the surface temperature and TPW bin and combines all emissivity classes as these become irrelevant. By not dividing profiles into emissivity bins, the retrieval can be more robust and might be the first one to run as we build the databases in the GPM era.

Version V1, S0 Status: Channel reduction for the S0 retrieval is being completed by Grant Petty where Tb offsets calculated from the difference of the observed Tbs and the Model computed Tbs are used. Options for running the GPROF2014 retrieval in S0 or S1 are completed in the retrieval code.

If we know something about the emissivity (I take this to mean that we are in an emissivity class with good covariance between channels), the retrieval will look at the appropriate surface temperature, TCWV, and Surface Classification for a match. For Version B2, the emissivity classes are simply the mean emissivity cluster for that quarter degree grid. Co-variance of the emissivities are still pending for future versions.

Finally, if we know the emissivity, then we again ignore the emissivity bin, but match only profiles with the correct emissivity – i.e., departures in the emissivity would be treated as departures in the T_b between observations and database entries. We'll call this the S2 retrievals and obviously need to add the emissivities to the database as well.

Since there are three options, we suggest that we always run two of them (either S0 & S1 or S1 and S2) to provide the difference between methods. Particularly over land, I think this will give us a robust indicator of the product robustness.

5.0 KNOWN LIMITATIONS

a) There are no profiles retrieved over snow covered land surfaces due to Satellite Radiometer matching with only the MRMS (ground radar) surface precipitation. At the time no profile of hydrometeors was available.

b) Light rain and drizzle in the high latitude are still poorly observed. Though we did increase the high latitude precipitation over ocean it probably is still low.

c) Precipitation phase at high elevations is often incorrect (frozen precipitation is reported as rain). As shown in the Olympex experiment winter higher elevation precipitation had the worng phase. The model (GANAL or ECMWF) 2 meter wet bulb temperature is used as the phase

discriminator, and the crude resolution (often 50km) cannot accurately capture the cold mountain temperatures.

d) Precipitation in coastal regions continue to be lower in quality. When the satellite pixel encompasses both land and water in the field-of-view (coast surface class), the microwave surface emissivity depends greatly on the relative percentages of each.

6.0 ALGORITHM IMPROVEMENTS – a History of GPROF for GPM

Transition to later algorithms with the GPM database: For the first GPM-based *a-priori* database, the radiometer algorithm team created an empirical database using DPR observed precipitation and GMI observations. Techniques that have been developed jointly with the X-cal team will be used to translate the observed GMI T_bs to equivalent T_b that would be observed by other constellation radiometers. This was done quickly and will ensure that a good product was available from the radiometers soon after launch. Subsequent versions relied on physically constructed solutions from the "combined algorithm" team. Physical solutions not only ensure consistency between radar and radiometer, but also the retrieved geophysical parameters ensure that the computed T_b for the constellation radiometers is fully consistent with the *a-priori* database. Since the "combined algorithm" product becomes the *a-priori* database for GMI as well as the radiometer constellation, the radiometer algorithm will always be one version behind the combined team.

The transition to "fully physical" retrievals: The first at-launch database as described above was empirical in nature. By this we understand that a radiative transfer computation using the retrieved rainfall profiles from DPR do not necessarily yield the T_b observed by GMI. The reasons for the differences can be many, including; incorrect assumptions about drop size distributions, cloud water contents, ice microphysics, or surface properties. In some cases, such as tropical oceans, we have already developed techniques to adjust retrieved parameters so as to be simultaneously consistent with radar and radiometer observations on TRMM. These regions have been quickly transitioned (in the first reprocessing) from empirical to physical within GPM as well. The combined algorithm, however, will not always be able to create physically consistent solutions between DPR and GMI. An example is a complex coastline where emissivity is not known or calculable. The combined algorithm in this case will use only DPR to create a solution, leaving the *a-priori* database needed by the radiometer to be empirical. Because of this, the radiometer algorithm plans on a phased approach, starting with an empirically constructed *a-priori* database and transitioning this database to a physical one as we understand specific surfaces. The degree to which various surfaces are physically understood is shown below under "Emissivity models".

Section 1.4 describes the changes to the algorithm and input data processing for GPM V5. The greatest change is probably the pixel to pixel Tb bias correction, but others were just as important.

Emissivity models: Over oceans, good emissivity models exist that allow "combined retrievals"

to produce physically consistent geophysical parameters. Over land, there are some surfaces where good knowledge exists (e.g. rain forests) while others (*e.g.*, semi-arid regions) still require significant work before a truly physical model of the emissivity can be constructed. In the GPM combined algorithm, two steps are defined. The first step requires only covariances of the emissivities among channels. When these covariances are well defined and reduce the emissivity problem to one or two degrees of freedom, then physical databases can be constructed that retrieve these one or two degrees of freedom. This will be done first as different investigators provide guidance on the best way to define these degrees of freedom for individual surfaces. From an algorithm point of view, this is the only step that is required. From a GPM science point of view, we want to further know how the free parameters are related to geophysical parameters that can then be assimilated into Land Surface Models (LSMs). Conversely, if the relationship between emissivity and emissivity covariance and land surface parameters is known, then LSMs can be used to limit the degrees of freedom that have to be retrieved with respect to the surface in much the same way that a weather forecast model can already be used to specific atmospheric temperature structure. First, in order to use the useful covariances among channels and then the entire LSM, the retrieval algorithm must be able to identify the specific surfaces of applicability. We will track the portion of the globe that uses these physical methods versus the default empirical methods as part of the algorithm development.

7.0 REFERENCES

Aires, Filipe, Frédéric Bernardo, Héléne Brogniez, Catherine Prigent, 2010: An innovative calibration method for the inversion of satellite observations, *J. of Appl. Meteorol. and Climatology*, **49**, 2458-2473, doi: 10.1175/2010JAMC2435.1.

Aires, F., Prigent, C., Bernardo, F., Jiménez, C., Saunders, R. and Brunel, P., 2011: A tool to estimate land-surface emissivities at microwave frequencies (TELSEM) for use in numerical weather prediction. *Q. J. of the Roy. Meteorol. Soc*., **137**: 690–699. doi: 10.1002/qj.803

Backus, G., and F. Gilbert, 1970: Uniqueness in the inversion of inaccurate gross earth data, *Philos. Trans. Roy. Soc. London*, A266, 123–192.

Berg, W., T. L'Ecuyer, and C. Kummerow, 2006. Rainfall climate regimes: The relationship of regional TRMM rainfall biases to the environment, *J. Appl. Meteor. Climatol.*, **45**, 434–454.

Boukabara, S.-A.; Fuzhong Weng; Quanhua Liu, 2007: Passive microwave remote sensing of extreme weather events using NOAA-18 AMSUA and MHS, *Geoscience and Remote Sensing, IEEE Transactions on* , **45**, 2228-2246, doi: 10.1109/TGRS.2007.898263.

Boukabara, S.-A.; Garrett, K.; Wanchun Chen; Iturbide-Sanchez, F.; Grassotti, C.; Kongoli, C.; Ruiyue Chen; Quanhua Liu; Banghua Yan; Fuzhong Weng; Ferraro, R.; Kleespies, T.J.; Huan Meng; 20011: MiRS: an all-weather 1DVAR satellite data assimilation and retrieval

system, *Geoscience and Remote Sensing, IEEE Transactions on* , **49**, 3249-3272, doi:10.1109/TGRS.2011.2158438

Hiley, M. J., M. S. Kulie, and R. Bennartz, 2011: Uncertainty Analysis for CloudSat Snowfall Retrievals. *J Appl Meteorol Clim*, **50,** 399-418.

Hollinger, J.P. 1989: *DMSP Special Sensor Microwave/Imager Calibration/Validation*. Final Report, Vol. I., Space Sensing Branch, Naval Research Laboratory, Washington D.C.

Kummerow, C., W.S. Olson and L. Giglio, 1996. A simplified scheme for obtaining precipitation and vertical hydrometeor profiles from passive microwave sensors, *IEEE, Trans on Geoscience and Remote Sensing,* **34**, 1213-1232, doi: 10.1109/36.536538.

Kummerow, C., W. Barnes, T. Kozu, J. Shiue and J. Simpson, 1998. The tropical rainfall measuring mission (TRMM) sensor package, *J. Atmos. Oceanic Technol.*, **15**, 809–817.

L'Ecuyer, T. S., G. L. Stephens, 2002: An estimation-based precipitation retrieval algorithm for attenuating radars. *J.Appl.Meteorol.,* **41**, 272-285.

Lorenc, A. C., 1986: Analysis methods for numerical weather prediction. *Quart. J. Roy. Meteor. Soc.*, **112**, 1177-1194.

Prigent, C., C., W. B. Rossow, and E. Matthews, 1997: Microwave land surface emissivities estimated from SSM/I observations. *J. Geophys. Res*., **102**, 21 867 – 21 890.

Prigent, C., E. Jaumouille, F. Chevallier, and F. Aires, 2008: A parameterization of the microwave land surface emissivity between 19 and 100 GHz, anchored to satellite-derived estimates*, IEEE Transaction on Geoscience and Remote Sensing* , **46**, 344-352, doi:10.1109/TGRS.2007.908881.

Rapp, A., M. Lebsock, C. Kummerow, 2009: On the Consequences of Resampling Microwave Radiometer Observations for Use in Retrieval Algorithms, *J. of Appl. Meteo. and Clim.,* **48**, 2242-2256, doi: 10.1175/2009JAMC2156.1.

Reynolds, R.W., T.M. Smith, C. Liu, D.B. Chelton, K.S. Casey, and M.G. Schlax, 2006: Daily high-resolution-blended analyses for sea surface temperature. *J. Climate,* **20,** 5473- 5496.

Sims, E.M. and G. Liu, 2015: A Parameterization of the Probability of Snow–Rain Transition. *J. Hydrometeor.,* **16**, 1466–1477, doi: 10.1175/JHM-D-14-0211.1.

Sudradjat, Arief, Nai-Yu Wang, Kaushik Gopalan, Ralph R. Ferraro, 2011: Prototyping a generic, unified land surface classification and screening methodology for GPM-era

microwave land precipitation retrieval algorithms, *J. Appl. Meteorol. and Climatology*, **50**, 1200-1211, doi: 10.1175/2010JAMC2572.1

Weng, F., B. Yan, and N.C. Grody, 2001: A microwave land emissivity model. *J. Geophys. Res.*, **106**, 20 115 – 20 123.

APPENDIX A

A.1 GPM CORE SATELITE

The GPM Core Spacecraft flies two precipitation instruments: the GPM Microwave Imager (GMI) and the Dual-frequency Precipitation Radar (DPR). Together, these instruments provide a unique capability for measuring precipitation falling as light rain or snow—conditions that have been difficult to detect using previous instruments. Compared to the earlier generation of instruments, the new capabilities of the GMI and DPR are enabled by the addition of high frequency channels (165.6 and 183.3 GHz) on the GMI, and the inclusion of a Ka-band (35.5 GHz) radar on the DPR.

A.1.1 GPM Microwave Imager

The GPM Microwave Imager (GMI) instrument is a multi-channel, conical-scanning, microwave radiometer serving an essential role in the near-global-coverage and frequent-revisit-time requirements of GPM (see Fig. A.1). The instrumentation enables the Core spacecraft to serve as both a 'precipitation standard' and as a 'radiometric standard' for the other GPM constellation members. The GMI is characterized by thirteen microwave channels ranging in frequency from

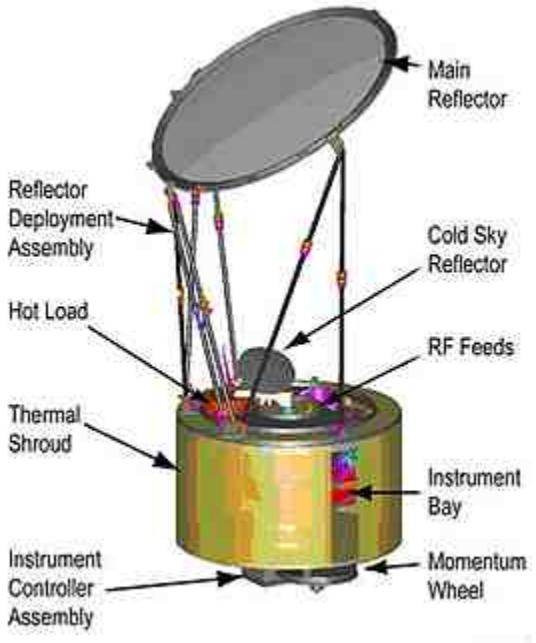

Fig. A.1. GMI instrument.

10 GHz to 183 GHz (see Table A.1). In addition to carrying channels similar to those on the Tropical Rainfall Measuring Mission (TRMM) Microwave Imager (TMI), the GMI carries four high frequency, millimeter-wave channels at about 166 GHz and 183 GHz. With a 1.2 m diameter antenna, the GMI will provide significantly improved spatial resolution over TMI. Launch date for the GPM core spacecraft was: February 27, 2014.

Table A.1. GMI performance characteristics.

Frequency (GHz)	Polarization	NEDT/ Reqmt (K)	Expected* NEDT	Expected Beam Efficiency (%)	Expected Calibration Uncert.	Resolution (km)
10.65	V/H	0.96	0.96	91.4	1.04	26
18.7	V/H	0.84	0.82	92.0	1.08	15
23.8	V	1.05	0.82	92.5	1.26	12
36.5	V/H	0.65	0.56	96.6	1.20	11
89.0	V/H	0.57	0.40	95.6	1.19	6
165.5	V/H	1.5	0.81	91.9	1.20	6
183.31±3	V	1.5	0.87	91.7	1.20	6
183.31±7	V	1.5	0.81	91.7	1.20	6

A.1.2 Dual-Frequency Precipitation Radar

One of the prime instruments for the GPM Core Observatory is the Dual-frequency Precipitation Radar (DPR). The DPR consists of a Ku-band precipitation radar (KuPR) and a Ka-band precipitation radar (KaPR). The KuPR (13.6 GHz) is an updated version of the highly successful unit flown on the TRMM mission. The KuPR and the KaPR were co-aligned on the GPM spacecraft bus such that the 5-km footprint location on the Earth are the same. Data collected from the KuPR and KaPR instruments provide the 3-dimensional observation providing an accurate estimation of rainfall rate to the scientific community. The DPR instrument is allocated 190 Kbps bandwidth over the 1553B spacecraft data bus. The collection of the DPR data is transmitted to the ground using the TDRSS multiple access (MA) and single access (SA) services. These Earth-pointing KuPR and KaPR instruments provides rain sensing over both land and ocean, both day and night. Top-level general design specifications are seen in Table A.2 and Fig. A.2.

The DPR is a spaceborne precipitation radar capable of making accurate rainfall measurements. The DPR is expected to be more sensitive than its TRMM predecessor especially in the measurement of light rainfall and snowfall in the high latitude regions. Rain/snow determination is accomplished by using the differential attenuation between the Ku-band and the Ka-band frequencies. The variable pulse repetition frequency (VPRF) technique increases the number of samples at each IFOV to realize a 0.2 mm/h sensitivity.

Table A.2. DPR performance characteristics.

Item	Swath Width (km)	Range Resolu-tion (m)	Spatial Resolu-tion (km Nadir)	Beam Width (deg)	Trans-mitter (SSA)	Peak Transmit Power (W)	Pulse Repe-tition Freq. (Hz)	Pulse Width	Beam #
KuPR	245	250	5	0.71	128	1000	4100 - 4400	2; 1.667 μs pulses	49
KaPR	120	250/500	5	0.71	128	140	4100 - 4400	2; 1.667 μs pulses in matched beams 2; 3.234 μs pulses in interlaced scans	49 (25 matched beams and 24 interlaced scans)

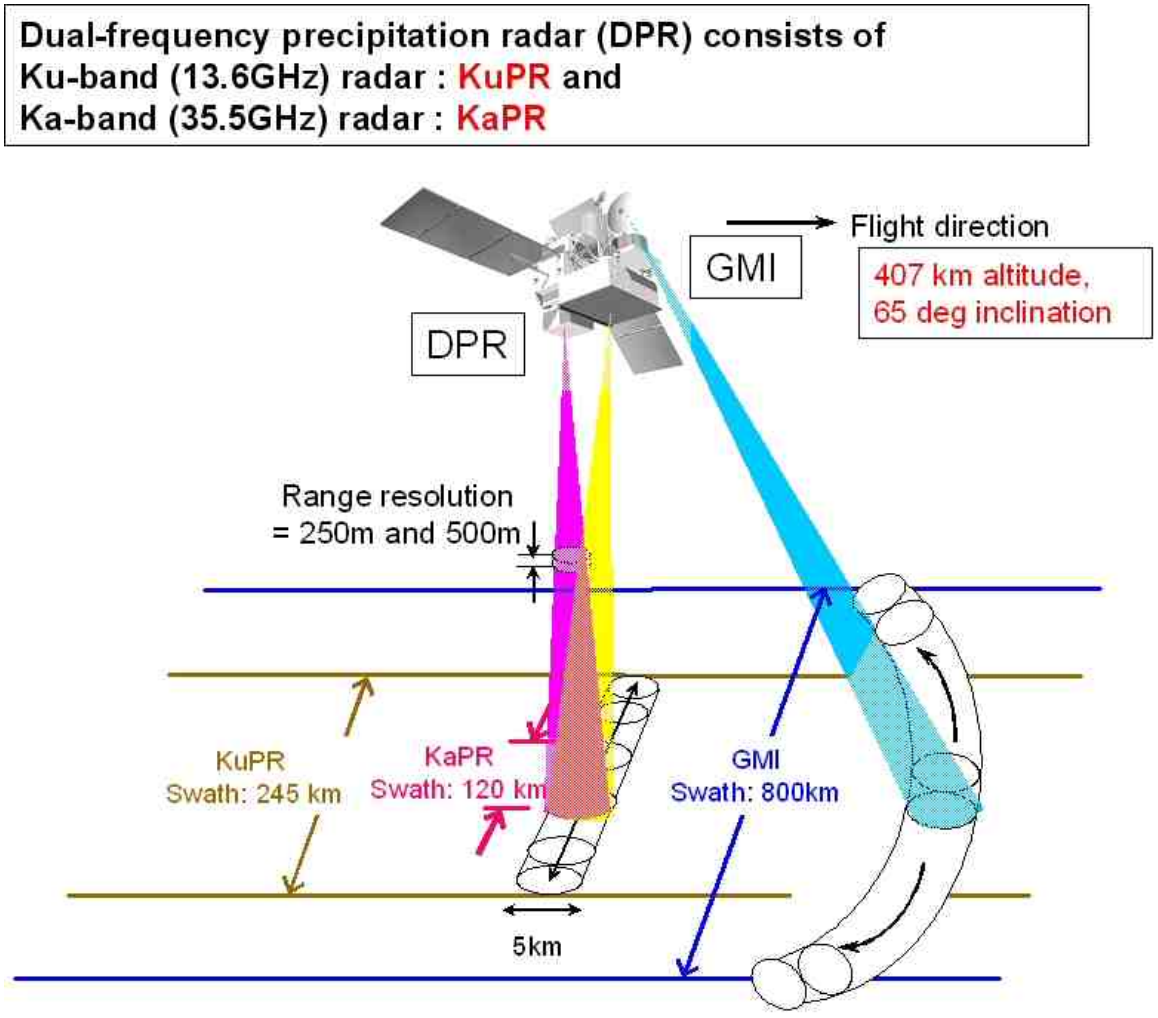

Fig. A2. GPM swath measurements.

A.2 The Advanced Microwave Scanning Radiometer 2

The Advanced Microwave Scanning Radiometer 2 (AMSR 2), which will fly on the GCOM-W1 platform is a sensor to observe microwave radiation at six different frequency bands ranging from 7 GHz to 89 GHz. AMSR 2 is designed to monitor Earth's hydrological cycle including sea surface temperature, cloud water, water vapor, precipitation, sea-ice, and soil moisture.

The antenna of the AMSR 2, which receives microwaves from the ground, arc scans the ground surface at a ratio of one turn every 1.5 seconds and observes an area approximately 1,450 kilometers wide in one scan. Using this scanning method, the AMSR 2 can observe over 99% of the Earth's area in just two days. The diameter of the antenna is about 2 m, making it the world's largest observation sensor aboard a satellite. The height of the rotating part is about 2.7 m and the weight is about 250 kg. The AMSR 2 can keep rotating such a large and heavy antenna at a speed of one turn per 1.5 s for 24 hours a day and more than five years without a minute of rest. Launch date: To be determined.

Table A.3. AMSR 2 performance characteristics

Orbit	Launch	Design life (yrs)	Local time (LTAN)	Swath width (km)	Antenna	Incidence angle (deg)
Sun Synchronous with 699.6km altitude (over equator)	JFY201	5	13:30	1450	2.0m offset parabola	Nominal 55

Table A.4. AMSR 2 Channel Set

Center Freq. (GHz)	Bandwidth (MHz)	Polarization	Beam Width (deg.) (ground res. [km])	Sampling Interval (km)
6.925/7.3	350	V/H	1.8 (35 x 62)	10
6.925/7.3	350	V/H	1.7 (34 x 58)	10
10.65	100	V/H	1.2 (24 x 42)	10
18.7	200	V/H	0.65 (14 x 22)	10
23.8	400	V/H	0.75 (15 x 26)	10
36.5	1000	V/H	0.35 (7 x 12)	10
89.0	3000	V/H	0.15 (3 x 5)	5

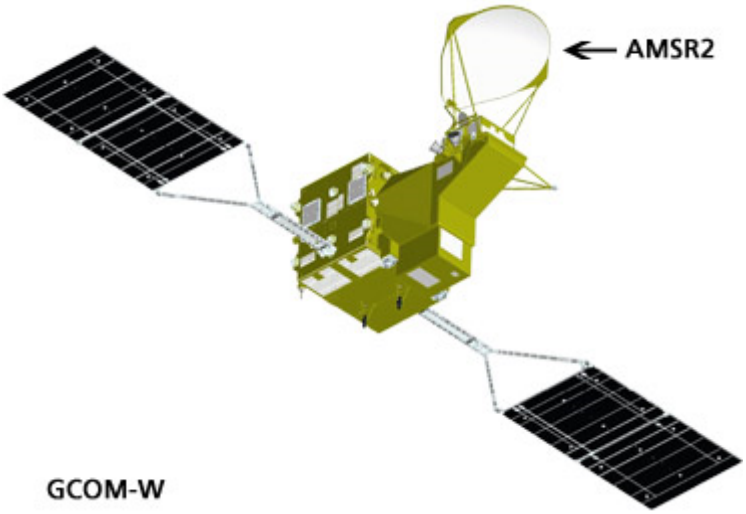

Fig. A.3. AMSR 2

A.3 MADRAS

MADRAS is a microwave imager, with conical scanning (incidence angle 56°), close to the SSM/I and TMI concepts. The main aim of the mission is the study of cloud systems. A frequency has been added (157 GHz) in order to study the high-level ice clouds associated with deep convective systems, and to serve as a window channel relative to the sounding instrument at 183 GHz.

Table A.5. Main characteristics of the MADRAS channels

Frequencies	Polarization	Pixel size (km)	Main use
18.7 GHz ± 100 MHz	H/V	40	ocean rain and surface wind
23.8 GHz ± 200 MHz	V	40	integrated water vapor
36.5 GHz ± 500 MHz	H/V	40	cloud liquid water
89 GHz ± 1350 MHz	H/V	10	convective rain areas
157 GHz ± 1350 MHz	H/V	6	cloud top ice

The main uses given here are only descriptive. In practice most of the products will be extracted from algorithms combining the different channels information. The resolutions are those expected in the different channels, accounting for the specification of 10 km given for the 89-GHz channel.

The general Geometry of scanning of the three instruments of the mission is represented in Fig. A.4.

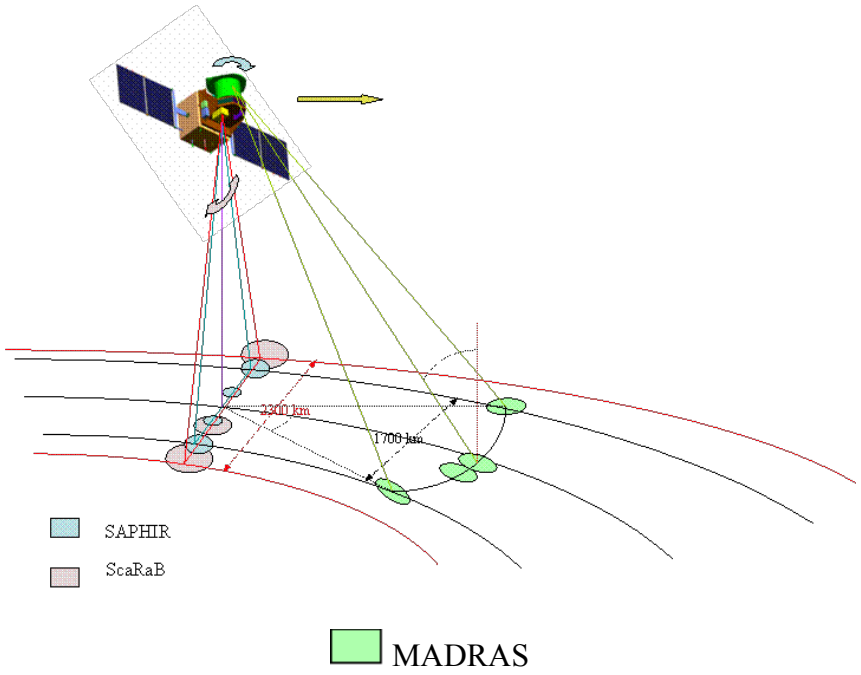

Fig. A.4. General configuration of the swath of the three instruments of Megha-Tropiques. Size of the footprints has been enhanced in order to show their geometric behavior.

Spectral characteristics include three instruments that compose the core payload of the mission: a microwave imager, a microwave water vapor sounder, a radiative budget radiometer. Preliminary studies have defined the main characteristics of these instruments. Launch date: Scheduled for the second half of 2010.

A.4 Sondeur Atmosphérique du Profil d'Humidité Intertropicale par Radiométrie

Sondeur Atmosphérique du Profil d'Humidité Intertropicale par Radiométrie (SAPHIR) is a sounding instrument with six channels near the absorption band of water vapor at 183 GHz. These channels provide relatively narrow weighting functions from the surface to about 10 km, allowing retrieving water vapor profiles in the cloud free troposphere. The scanning is cross-track, up to an incidence angle of 50°. The resolution at nadir is of 10 km.

The atmospheric opacity spectrum (see Fig. A.5) shows a first water vapor absorption line centered at 22.235 GHz, and a second one at 183.31 GHz (pure rotation line). Between these two lines, the water vapor continuum slowly increases absorption by the atmosphere with frequency. The first water vapor line is too low to permit profiling, and its partial transparency is used to obtain the total columnar content. The second line is high enough to enable sounding in the first 10-12 km of the atmosphere. The sounding principle consists of selecting channels at different frequencies inside the absorption line, in order to obtain a maximal sensitivity to humidity at different heights. Previous microwave sounders are SSMT2 and AMSU-B, which are operational instruments and have three channels within the 183.31 GHz absorption line (at

±1, ±3 and ±7 GHz), and two window channels, at 150 and 89 GHz. These additional channels give information on the surface and near surface.

Table A.6. Channel selection for SAPHIR on board Megha/Tropiques.

Channel	Center Freq. (GHz)	Bandwidth (MHz)	Sensitivity (K)	Polarization
S1	183.31±0.2	200	1.82	H
S2	183.31±1.1	350	1.01	H
S3	183.31±2.7	500	0.93	H
S4	183.31±4.0	700	0.88	H
S5	183.31±6.6	1200	0.81	H
S6	183.31±11.0	2000	0.73	H

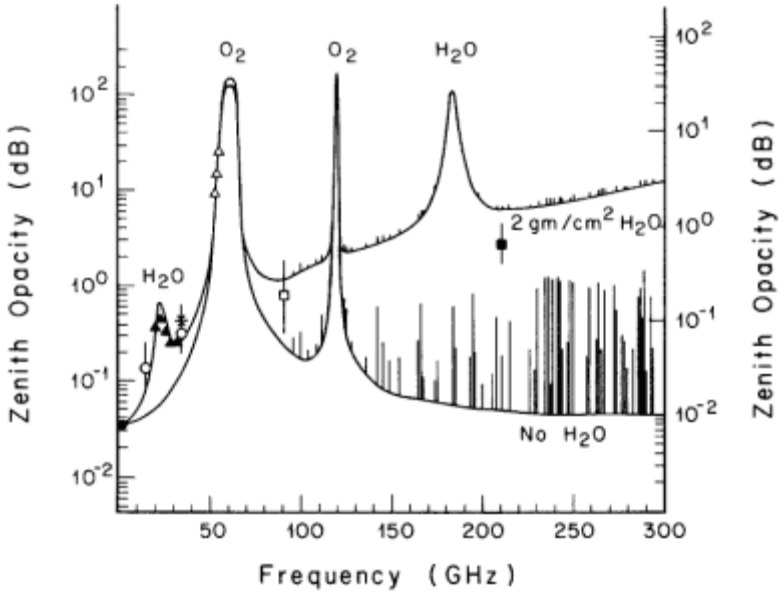

Fig. A.5. The atmospheric opacity for a US standard atmosphere.

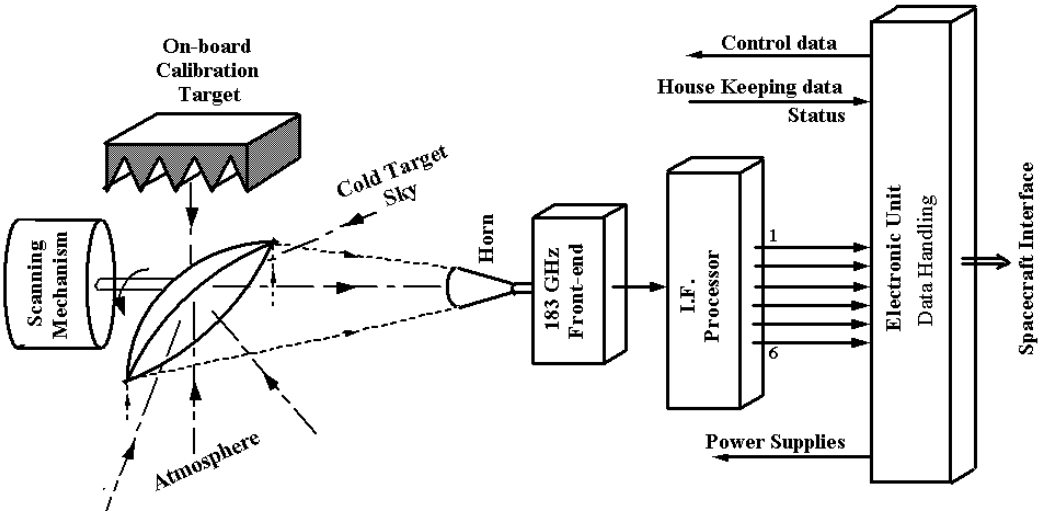

Fig. A.6. SAPHIR instrument.

A.5 Special Sensor Microwave Imager/Sounder

The Special Sensor Microwave Imager/Sounder (SSMIS) is a conically scanning passive microwave radiometer with a 53.1° earth incidence angle sensing upwelling microwave radiation at 24 channels covering a wide range of frequencies from 19-183 GHz. The Level 1C dataset contains only 11 of these channels, which are most relevant to sensing precipitation. Data is collected along an active scan of 144 degrees across track producing a swath width on the ground of 1707 km. The first of five sensors were launched on board DMSP F16 on October 18, 2003. The SSMIS is a joint US Air Force/Navy multi-channel passive microwave sensor that combines and extends the imaging and sounding capabilities of three separate DMSP microwave sensors including the SSM/T, SSM/T2, and SSM/I. It was built by Northrup-Grumman Electronic Systems.

Table A.7. SSMIS characteristics from the Algorithm and Data User Manual for SSMIS (2002). (Note: The channels in the Level 1C dataset are a subset of the full SSMIS channel complement.)

Center Freq. (GHz)	Polarization	Bandwidth (MHz)	IFOV (km x km)	EFOV* (km x km)	Sensitivity (K)
19.35	V/H	350	73x47	45x74	0.35
22.235	V	410	73x47	45x74	0.45
37.0	V/H	160	41x31	28x45	0.22
91.665	V/H	1410	14x13	13x16	0.19
150	H	1640	14x13	13x16	0.53
183.311 ± 1	H	510	14x13	13x16	0.38
183.311 ± 3	H	1020	14x13	13x16	0.39
183.311 ± 7	H	1530	14x13	13x16	0.56

*EFOV values are km along scan x km across scan.

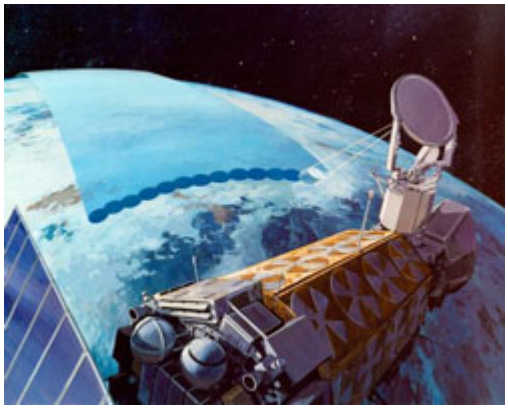

Fig. A.7. SSMIS.

A.6 WindSat

WindSat is a multi-frequency polarimetric microwave radiometer designed to demonstrate the capability of polarimetric microwave radiometry to measure the ocean surface wind vector from space. It has 22 channels operating at five frequencies. All frequencies have both V and H polarizations and three of the channels also have ±45, left-hand circular and right-hand circular polarizations. The instrument scans both before and after, and while some frequency bands have a swath width greater that 1200 km, the common swath width is approximately 950 km (68° of scan angle) and the aft common swath is 350 km (23° of scan angle). It was launched on board the U.S. Department of Defense Coriolis satellite on January 6, 2003 into an 840 km circular sun-synchronous orbit.

Table A.8. WindSat performance characteristics.

Center Freq. (GHz)	Polarization	Bandwidth (MHz)	Sensitivity (K)	IFOV (km x km)	Earth Incidence Angle (deg)
6.8	V/H	125	0.48	60x40	53.5
10.7	V/H/±45/L/R	300	0.37	38x25	49.9
18.7	V/H/±45/L/R	750	0.39	27x16	55.3
23.8	V/H	500	0.55	20x12	53.0
37.0	V/H/±45/L/R	2000	0.45	13x8	53.0

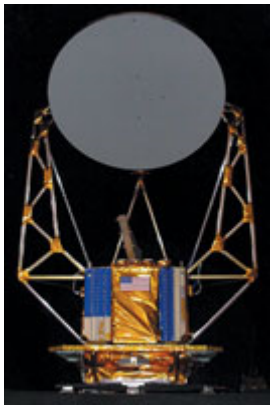

Fig. A.8. WindSat.

A.7 Advanced Microwave Scanning Radiometer-E

The Advanced Microwave Scanning Radiometer-E (AMSR-E) is a conically scanning total power passive microwave radiometer sensing microwave radiation (brightness temperatures) at 12 channels and 6 frequencies ranging from 6.9 to 89.0 GHz. Horizontally and vertically polarized radiation are measured separately at each frequency. There are two separate horns at 89 GHz, one being slightly offset from the centerline of the feedhorn array. *(As of 25 October 2004,*

there are no data from the 89-GHz horn A. The science algorithms have been modified to take this into account).

The AMSR-E instrument (Fig. A.9) modified from the design used for the ADEOS-II AMSR, has an offset parabolic reflector 1.6 meters in diameter. Figure A.10 shows the Aqua satellite with AMSR-E mounted in front. The atmospheric radiation is focused by the main reflector into an array of six feedhorns (Fig. A.11), which then feed the radiation to the detectors.

Fig. A.9. AMSR-E Instrument.

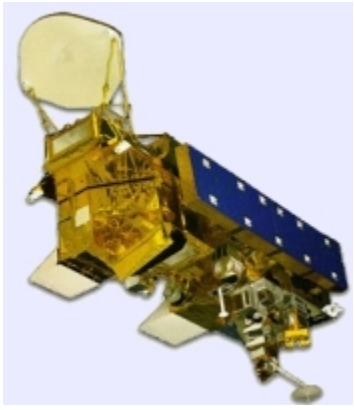

Fig. A.10. AMSR-E on the Aqua Satellite.

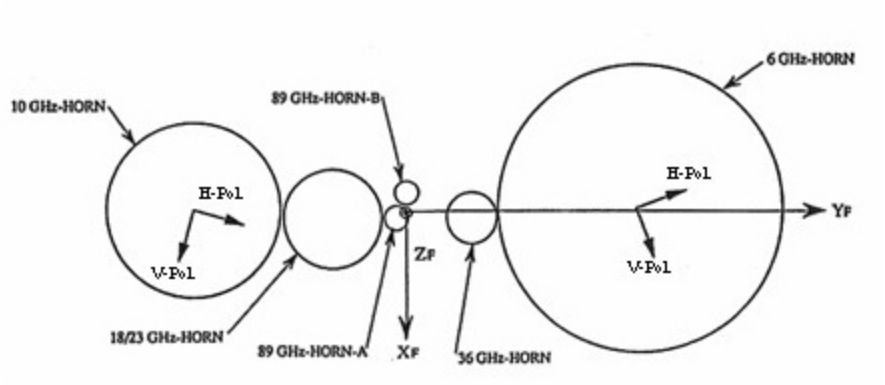

Fig. A.11. AMSR-E Horn Configuration.

A cold load reflector and a warm load are mounted on the transfer assembly shaft and do not rotate with the drum assembly. They are positioned off axis such that they pass between the feedhorn array and the parabolic reflector, occulting it once each scan. The cold load reflector reflects cold sky radiation into the feedhorn array thus serving, along with the warm load, as calibration references for the AMSR-E. Calibration of the radiometers is essential for collection of useful data. Corrections for spillover and antenna pattern effects are incorporated in the data processing algorithms.

The AMSR-E rotates continuously about an axis parallel to the local spacecraft vertical at 40 revolutions per minute (rpm). At an altitude of 705 km, it measures the upwelling scene brightness temperatures over an angular sector of ±61 degrees about the sub-satellite track, resulting in a swath width of 1445 km.

During a period of 1.5 seconds the spacecraft sub-satellite point travels 10 km. Even though the instantaneous field-of-view for each channel is different, active scene measurements are recorded at equal intervals of 10 km (5 km for the 89-GHz channels) along the scan. The half cone angle at which the reflector is fixed is 47.4°, which results in an Earth incidence angle of 55.0°. Launch date: May 4, 2002. Table A.9 lists the pertinent performance characteristics.

Table A.9. AMSR-E performance characteristics.

Center Freq. (GHz)	Bandwidth (MHz)	Sensitivity (K)	Mean Spatial Resol-ution (km)	IFOV (km x km)	Sampling Rate (km x km)	Integration Time (m/sec)	Main Beam Efficiency (%)	Beam Width (deg.)
6.925	350	0.3	56	74 x 43	10 x 10	2.6	95.3	2.2
10.65	100	0.6	38	51 x 30	10 x 10	2.6	95.0	1.4
18.7	200	0.6	21	27 x 16	10 x 10	2.6	96.3	0.8
23.8	400	0.6	24	31 x 18	10 x 10	2.6	96.4	0.9
36.5	1000	0.6	12	14 x 8	10 x 10	2.6	95.3	0.4
89.0	3000	1.1	5.4	6 x 4	5 x 5	1.3	96.0	0.18

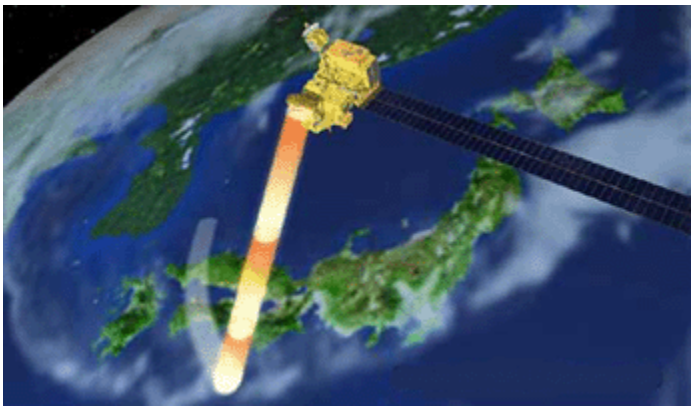

Fig. A.12. AMSR-E.

A.8 Advanced Microwave Sounding Unit

The Advanced Microwave Sounding Unit (AMSU) is a multi-channel microwave radiometer installed on meteorological satellites. The instrument examines several bands of microwave radiation from the atmosphere to perform atmospheric sounding of temperature and moisture levels. AMSU data is used extensively in weather prediction. Brightness temperatures are processed as quickly as possible and sent to numerical weather prediction (NWP) centers around the world. This data helps keep the assessment of the current state of the atmosphere correct, which in turn helps make predictions more accurate. Long-term AMSU records are also used in studies of climate.

The AMSU has two sub-instruments, AMSU-A and AMSU-B. AMSU-A has 15 channels between 23.8 and 89 GHz, and is used primarily for measuring atmospheric temperatures (known as "temperature sounding"). It has a ground resolution near nadir of 45 km. AMSU-B, with five channels between 89 and 183.3 GHz, has a spatial resolution near nadir of 15 km and is primarily intended for moisture sounding. Spot size of both sub-instruments becomes larger and more elongated toward the edges of the swath. When the two instruments are used together, there are roughly nine AMSU-B fields-of-view in a 3x3 array corresponding to each AMSU-A field-of-view. This reflects the higher spatial variability of water vapor compared to temperature. HIRS/3 infrared sounders with the same spatial resolution as AMSU-B are also included on NOAA 15-17 satellites and are used together with AMSU-A and AMSU-B. Together the three instruments form ATOVS, the Advanced TIROS Operational Vertical Sounder.

The Aqua and MetOp AMSU-A instruments are 15-channel microwave sounders designed primarily to obtain temperature profiles in the upper atmosphere (especially the stratosphere) and to provide a cloud-filtering capability for tropospheric temperature observations. The EOS AMSU-A is part of a closely coupled triplet of instruments that include the AIRS and HSB. The MetOp AMSU-A similarly works with HIRS, IASI, and MHS. MHS and HSB are variants on AMSU-B.

Table A.10. Radiometric characteristics of the AMSU-A.

Channel	Freq. (GHz)	Polarization (at nadir)	Band #	Sensitivity (K)	Primary Function
1	23.8	V	1	0.30	Water vapor burden
2	31.4	V	1	0.30	Water vapor burden
3	50.3	V	1	0.40	Water vapor burden
4	52.8	V	1	0.25	Water vapor burden
5	53.596 ± 0.115	H	2	0.25	Tropospheric Temperature
6	54.4	H	1	0.25	Tropospheric Temperature
7	54.94	V	1	0.25	Tropospheric Temperature
8	55.5	H	1	0.25	Tropospheric Temperature
9	57.290	H	1	0.25	Stratospheric Temperature
10	57.290 ± 0.217	H	2	0.40	Stratospheric Temperature
11	57.290 ± 0.3222 ± 0.048	H	4	0.40	Stratospheric Temperature
12	57.290 ± 0.3222 ± 0.022	H	4	0.60	Stratospheric Temperature
13	57.290 ± 0.3222 ± 0.010	H	4	0.80	Stratospheric Temperature
14	57.290 ± 0.3222 ± 0.0045	H	4	1.20	Stratospheric Temperature
15	89.0	V	1	0.60	Cloud top/snow

Table A.11. Radiometric characteristics of the AMSU-B.

Channel	Freq. (GHz)	Polarization (at nadir)	Band #	Sensitivity (K)
16	89.9 ± 0.9	V	2	0.37
17	150 ± 0.9	V	2	0.84
18	183.31 ± 1.00	V	2	1.06
19	183.31 ± 3.00	V	2	0.70
20	183.31 ± 7.00	V	2	0.60

A.9 TRMM Microwave Imager

The TRMM Microwave Imager (TMI) is a nine-channel passive microwave radiometer based upon the Special Sensor Microwave/Imager (SSM/I), which has been flying aboard the U.S. Defense Meteorological Satellite Program (DMSP) satellites since 1987. The key differences are the addition of a pair of 10.7-GHz channels with horizontal and vertical polarizations and a frequency change of the water vapor channel from 22.235 to 21.3 GHz. This change off the center of the water vapor line was made in order to avoid saturation in the tropical orbit of TRMM. Table A.12 presents the performance characteristics of the nine TMI channels. The increased spatial resolution evident in Table A.12 is due to the lower orbit of the TRMM satellite with respect to the DMSP rather than sensor differences.

The TMI antenna (Fig. A.13) is an offset parabola, with an aperture size of 61 cm (projected along the propagation direction) and a focal length of 50.8 cm. The antenna beam views the earth's surface with a nadir angle of 498, which results in an incident angle of 52.88 at the earth's surface. The TMI antenna rotates about a nadir axis at a constant speed of 31.6 rpm. The rotation draws a circle on the earth's surface. Only 1308 of the forward sector of the complete circle is used for taking data. The rest is used for calibrations and other instrument housekeeping purposes. From the TRMM orbit, the 130 scanned sector yields a swath width of 758.5 km shown in Fig. A.14. During each complete revolution (*i.e.*, a scan period of about 1.9 s), the sub-satellite point advances a distance *d* of 13.9 km. Since the smallest footprint (85.5-GHz channels) size is only 6.9 km (down-track direction) by 4.6 km (cross-track direction), there is a gap of 7.0 km between successive scans. However, this is the only frequency where there is a small gap. For all higher-frequency channels, footprints from successive scans overlap the previous scans. Launch date: 1997, active.

Table A.12. TMI performance characteristics.

Channel	Center Freq. (GHz)	Polari-zation	Bandwidth (MHz)	Sensitivity (K)	IFOV (km x km)	Sampling Interval (km x km)	Integr-ation Time (m/sec)	Main Beam Effic-iency (%)	Beam width (deg)
1	10.65	V	100	0.63	63 x 37	13.9x9.1	6.6	93	3.68
2	10.65	H	100	0.54	63 x 37	13.9x9.1	6.6	93	3.75
3	19.35	V	500	0.50	30 x 18	13.9x9.1	6.6	96	1.90
4	19.35	H	500	0.47	30 x 18	13.9x9.1	6.6	96	1.88
5	21.3	V	200	0.71	23 x 18	13.9x9.1	6.6	98	1.70
6	37.0	V	2000	0.36	16 x 9	13.9x9.1	6.6	91	1.00
7	37.0	H	2000	0.31	16 x 9	13.9x9.1	6.6	92	1.00
8	85.5	V	3000	0.52	7 x 5	13.9x4.6	3.3	82	0.42
9	85.5	H	3000	0.93	7 x 5	13.9x4.6	3.3	85	0.43

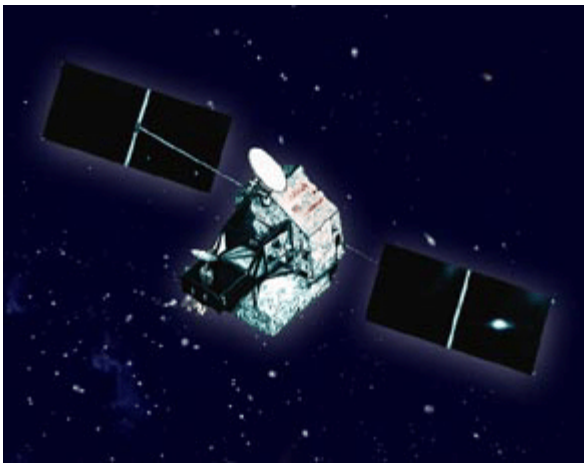

Fig. A.13. TMI.

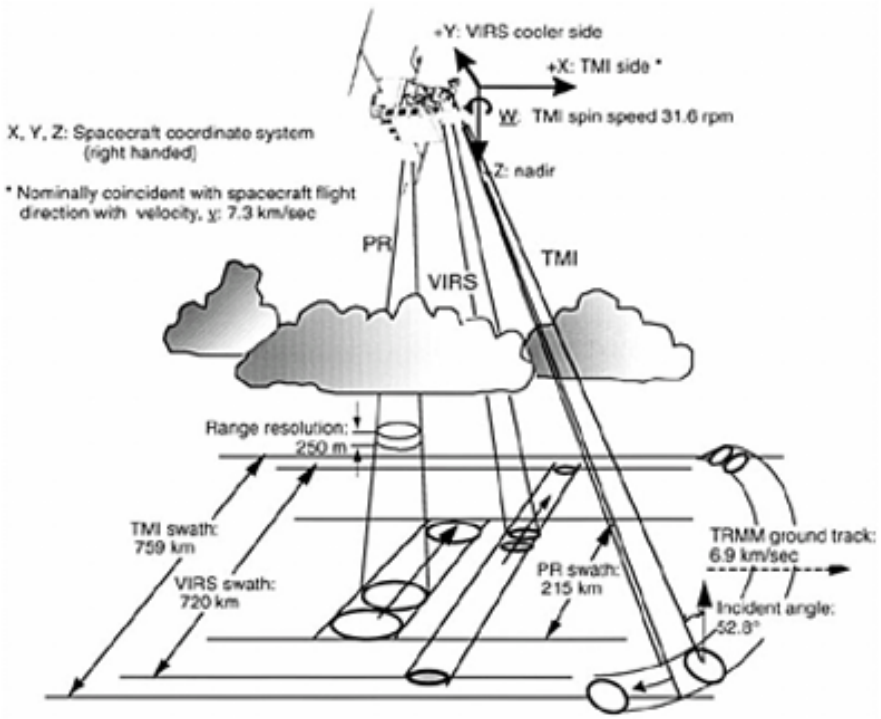

FIG. 1. Schematic view of the scan geometries of the three TRMM primary rainfall sensors: TMI, PR, and VIRS.

Fig. A.14. Schematic view of the scan geometries of the three TRMM primary rainfall sensors: TMI, PR, and VIRS. Figure provided by Kummerow *et al.* (1998).

A.10 Special Sensor Microwave/Imager

The Special Sensor Microwave/Imager (SSM/I) is a seven-channel, four-frequency, linearly polarized passive microwave radiometric system. The instrument measures surface/atmospheric microwave T_bs at 19.35, 22.235, 37.0 and 85.5 GHz. The four frequencies are sampled in both horizontal and vertical polarizations, except the 22 GHz, which is sampled in the vertical only.

The SSM/I has been a very successful instrument, superseding the across-track and Dicke radiometer designs of previous systems. Its combination of constant-angle rotary-scanning and total power radiometer design has become standard for passive microwave imagers, (*e.g.,* TRMM Microwave Imager, AMSR). Information within the SSM/I T_bs measurements allow the retrieval of four important meteorological parameters over the ocean: near-surface wind speed (note scalar not vector), total columnar water vapor, total columnar cloud liquid water (liquid water path) and precipitation. However, accurate and quantitative measurement of these parameters from the SSM/I T_bs is a non-trivial task. Variations within the meteorological parameters significantly modify the T_bs. As well as open ocean retrievals, it is also possible to retrieve quantitatively reliable information on sea ice, land snow cover and over-land precipitation.

The instrument is flown onboard the United States Air Force Defense Meteorological Satellite Program (DMSP) Block 5D-2 spacecraft. These are in circular or near-circular Sun-synchronous and near-polar orbits at altitudes of 833 km with inclinations of 98.8° and orbital periods of 102.0 minutes, each making 14.1 full orbits per day. The scan direction is from the left to the right with the active scene measurements lying ±51.2 degrees about when looking in the F8 forward (F10-F15) or aft (F8) direction of the spacecraft travel. This results in a nominal swath width of 1394 km allowing frequent ground coverage, especially at higher latitudes. All parts of the globe at latitudes greater than 58° are covered at least twice daily except for small unmeasured circular sectors of 2.4° about the poles. Extreme polar regions (> 72° N or S) receive coverage from two or more overpasses from both the ascending and descending orbits each day.

The spin rate of the SSM/I provides a period of 1.9 s during which the DMSP spacecraft sub-satellite point travels 12.5 km. Each scan 128 discrete, uniformly spaced radiometric samples are taken at the two 85-GHz channels and, on alternate scans, 64-discrete samples are taken at the remaining five lower frequency channels. The resolution is determined by the Nyquist limit and the Earth's surface contribution of 3-dB bandwidth of the signal at a given frequency (see Table A.13). The radiometer direction intersects the Earth's surface at a nominal incidence angle of 53.1 degrees, as measured from the local Earth normal.

Table A.13. Radiometric performance characteristics of the SSM/I (Hollinger 1989).

Center Freq. (GHz)	**Polarization**	**IFOV (km x km)**	**Spatial Sampling (km)**	**Sensitivity (K)**
19.35	H	69x43	25	0.42
19.35	V	69x43	25	0.45
22.235	V	50x40	25	0.74
37.0	H	37x28	25	0.38
37.0	V	37x28	25	0.37
85.5	H	15x13	12.5	0.73
85.5	V	15x13	12.5	0.69

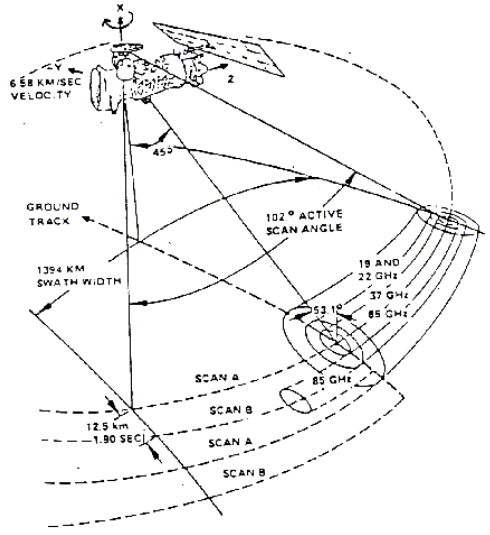

Fig. A15. The scan geometry of the SSM/I.

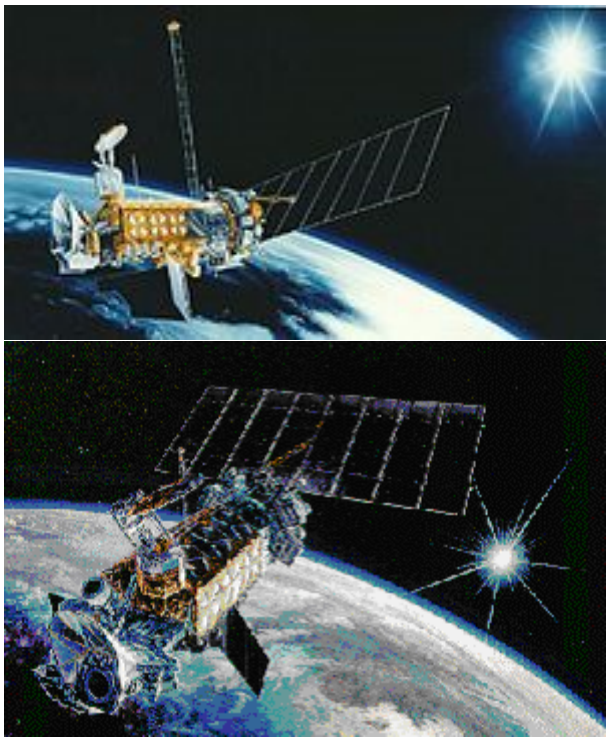

Fig. A.16. SSM/I.

A.11 Advanced Technology Microwave Sounder

The Advanced Technology Microwave Sounder (ATMS) will operate in conjunction with the Cross-track Infrared Sounder (CrIS) to profile atmospheric temperature and moisture. The ATMS is the next generation cross-track microwave sounder that will combine the capabilities of

current generation microwave temperature sounders (Advanced Microwave Sounding Unit – AMSU-A) and microwave humidity sounders (AMSU-B) that are flying on NOAA's Polar Operational Environmental Satellites (POES). The ATMS draws its heritage directly from AMSU-A/B, but with reduced volume, mass and power. The ATMS has 22 microwave channels to provide temperature and moisture sounding capabilities. Sounding data from CrIS and ATMS will be combined to construct atmospheric temperature profiles at 1 K accuracy for 1 km layers in the troposphere and moisture profiles accurate to 15% for 2 km layers. Higher (spatial, temporal and spectral) resolution and more accurate sounding data from CrIS and ATMS will support continuing advances in data assimilation systems and Numerical Weather Prediction (NWP) models to improve short- to medium-range weather forecasts.

Both CrIS and ATMS (CrIMSS) are selected to fly on the National Polar-orbiting Operational Environmental Satellite System (NPOESS) spacecraft, combining both cross-track infrared and microwave sensors aboard the NPOESS satellite. Expected NPP launch year is 2011.

Table A.14. Instrument characteristics of the ATMS.

Channel	Center Freq. (GHz)	Bandwidth (GHz)	Center Freq. Stability (MHz)	Temp. Sensitivity (K)
1	23.8	0.27	<10	0.7
2	31.4	0.18	<10	0.8
3	50.3	0.18	<10	0.9
4	51.76	0.4	<5	0.7
5	52.8	0.4	<5	0.7
6	53.596±0.115	0.17	<5	0.7
7	54.4	0.4	<5	0.7
8	54.94	0.4	<10	0.7
9	55.5	0.33	<10	0.7
10	57.290344	0.33	<0.5	0.75
11	57.290344±0.217	0.078	<0.5	1.2
12	57.290344±0.3222±0.048	0.036	<1.2	1.2
13	57.290344±0.03222±0.022	0.016	<1.6	1.5
14	57.290344±0.03222±0.010	0.008	<0.5	2.4
15	57.290344±0.03222±0.0045	0.003	<0.5	3.6
16	88.2	2.0	<200	0.5
17	165.5	3.0	<200	0.6
18	183.31±7	2.0	<30	0.8
19	183.31±4.5	2.0	<30	0.8
20	183.31±3	1.0	<30	0.8
21	183.31±1.8	1.0	<30	0.8
22	183.31±1	0.5	<30	0.9

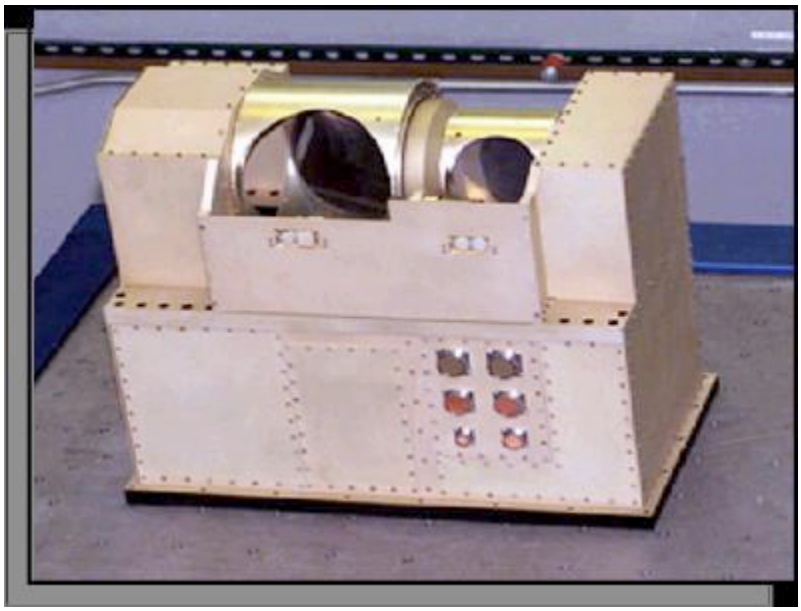

Fig. A.17. ATMS Instrument.

A.12 Microwave Humidity Sounder

MHS - The Microwave Humidity Sounder (MHS) is one of the European instruments carried on MetOp-A. MHS is a five-channel, total power, microwave radiometer designed to scan through the atmosphere to measure the apparent upwelling microwave radiation from the Earth at specific frequency bands. Since humidity in the atmosphere (ice, cloud cover, rain and snow) attenuate microwave radiation emitted from the surface of the Earth, it is possible, from the observations made by MHS, to derive a detailed picture of atmospheric humidity with the different channels relating to different altitudes. Temperature at the surface of the Earth can also be determined.

MHS works in conjunction with four of the U.S. instruments provided by the National Oceanic and Atmospheric Administration (NOAA), namely the Advanced Microwave Sounding Unit–A1 (AMSU-A1), the Advanced Microwave Sounding Unit–A2 (AMSU-A2), the Advanced Very High Resolution Radiometer (AVHRR) and the High Resolution Infrared Sounder (HIRS). Along with these instruments, MHS is already in operation on the NOAA-18 satellite, which was launched in May 2005, and it also forms a part of the payload on NOAA-N' launched in 2008. MHS represents a significant enhancement in performance over the AMSU-B currently flying on the earlier NOAA-15,-16 and -17 satellites.

In conjunction with these U.S. instruments, the MHS instrument will provide improved data for weather prediction models with a resulting improvement in weather forecasting. MHS is intended primarily for the measurement of atmospheric humidity. It will measure cloud liquid water content. Furthermore, it will provide qualitative estimates of precipitation rate.

MHS helps to ensure the continuous and improved availability of operational meteorological observations from polar orbit whilst providing Europe with an enhanced capability for the routine observation of the Earth from space, and in particular, to further increase Europe's capability for long-term climate monitoring.

MHS instrument is a five-channel, self-calibrating microwave rotating radiometer on the nadir-facing side of the MetOp-A satellite and is designed to scan perpendicular to the direction flight (across track) at a rate of 2.67 s per scan. The swath width of the scan is approximately ±50°. The scan is synchronized with the AMSU-A1 and A2 instruments, with MHS performing three scan cycles for every one performed by the AMSU instruments.

The MHS incorporates four receiver chains at 89 GHz, 157 GHz and 190 GHz, with the 183-GHz data sampled in two discrete bands to provide the five channels. The fifth channel is achieved by splitting the 183.311 GHz signal into two channels, each with a different bandwidth.

Table A.15. Channel characteristics of the MHS.

Channel	Center Freq. (GHz)
1	89.0
2	157.0
3	183.311±1.0
4	183.311 ± 3.0
5	190.31

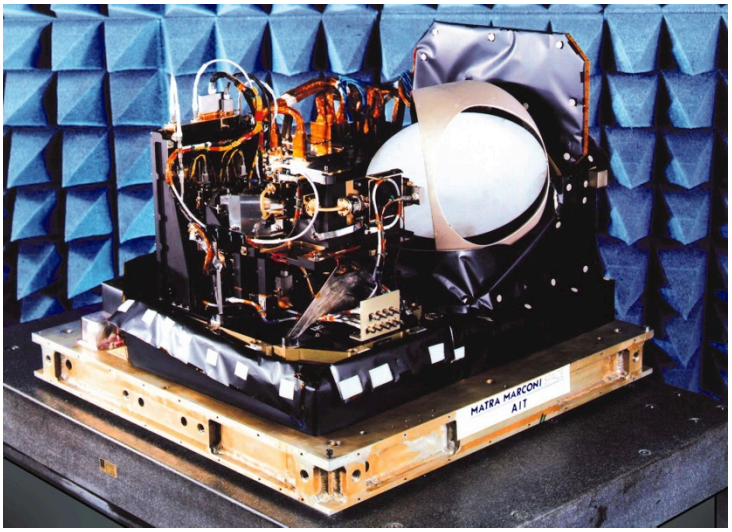

Fig. A.18. MHS instrument.